![U.S.NRC logo]

U.S.NRC
United States Nuclear Regulatory Commission

Protecting People and the Environment

Analysis of Experimental Data for High Burnup BWR Spent Fuel Isotopic Validation – SVEA-96 and GE14 Assembly Designs

Office of Nuclear Regulatory Research

AVAILABILITY OF REFERENCE MATERIALS
IN NRC PUBLICATIONS

NRC Reference Material

As of November 1999, you may electronically access NUREG-series publications and other NRC records at NRC's Public Electronic Reading Room at http://www.nrc.gov/reading-rm.html. Publicly released records include, to name a few, NUREG-series publications; *Federal Register* notices; applicant, licensee, and vendor documents and correspondence; NRC correspondence and internal memoranda; bulletins and information notices; inspection and investigative reports; licensee event reports; and Commission papers and their attachments.

NRC publications in the NUREG series, NRC regulations, and Title 10, "Energy," in the *Code of Federal Regulations* may also be purchased from one of these two sources.
1. The Superintendent of Documents
    U.S. Government Printing Office Mail Stop SSOP
    Washington, DC 20402–0001
    Internet: bookstore.gpo.gov
    Telephone: 202-512-1800
    Fax: 202-512-2250
2. The National Technical Information Service
    Springfield, VA 22161–0002
    www.ntis.gov
    1–800–553–6847 or, locally, 703–605–6000

A single copy of each NRC draft report for comment is available free, to the extent of supply, upon written request as follows:
Address: U.S. Nuclear Regulatory Commission
          Office of Administration
          Publications Branch
          Washington, DC 20555-0001
E-mail: DISTRIBUTION.RESOURCE@NRC.GOV
Facsimile: 301–415–2289

Some publications in the NUREG series that are posted at NRC's Web site address http://www.nrc.gov/reading-rm/doc-collections/nuregs are updated periodically and may differ from the last printed version. Although references to material found on a Web site bear the date the material was accessed, the material available on the date cited may subsequently be removed from the site.

Non-NRC Reference Material

Documents available from public and special technical libraries include all open literature items, such as books, journal articles, transactions, *Federal Register* notices, Federal and State legislation, and congressional reports. Such documents as theses, dissertations, foreign reports and translations, and non-NRC conference proceedings may be purchased from their sponsoring organization.

Copies of industry codes and standards used in a substantive manner in the NRC regulatory process are maintained at—
        The NRC Technical Library
        Two White Flint North
        11545 Rockville Pike
        Rockville, MD 20852–2738

These standards are available in the library for reference use by the public. Codes and standards are usually copyrighted and may be purchased from the originating organization or, if they are American National Standards, from—
        American National Standards Institute
        11 West 42nd Street
        New York, NY 10036–8002
        www.ansi.org
        212–642–4900

Analysis of Experimental Data for High Burnup BWR Spent Fuel Isotopic Validation – SVEA-96 and GE14 Assembly Designs

Prepared by:
H. J. Smith
I. C. Gauld
U. Mertyurek

Oak Ridge National Laboratory
Managed by UT-Battelle, LLC
Oak Ridge, TN 37831-6170

Mourad Aissa, NRC Project Manager

Office of Nuclear Regulatory Research

ABSTRACT

This report describes experimental radiochemical assay data, recently acquired under two international collaboration programs, for the isotopic compositions in high burnup spent nuclear fuel from modern boiling water reactor (BWR) assemblies. The Belgian MALIBU extension program provides measured data for isotopic contents of more than 50 nuclides in spent fuel samples selected from a SVEA-96 (10×10) Optima fuel assembly with burnups between 59 and 63 GWd/MTU. An experimental program in Spain provides additional isotopic data for more than 60 nuclides in samples selected from a GE14 (10×10) fuel assembly that cover a burnup range 38 to 56 GWd/MTU. These samples were selected from different axial elevations of a fuel rod, representing therefore a wide range of moderator void conditions. The measurement data include concentrations of actinides and fission products important to nuclear decay heat, radiological sources, and nuclear criticality safety. These data are essential for validation of the computational models used to calculate fuel isotopic concentrations and activities applied in reactor and spent nuclear fuel safety studies. Computational benchmark analyses using the measurements are performed with the TRITON two-dimensional depletion sequence in the SCALE 6.1 computer code system and ENDF/B-VII-based nuclear data libraries. These measurements represent an important contribution to the code benchmark database by providing data for modern BWR assembly designs and operating conditions representative of currently operating reactors.

CONTENTS

LIST OF FIGURES

LIST OF TABLES

Page

ACKNOWLEDGMENTS

LIST OF ACRONYMS AND UNITS

BWR	boiling water reactor
C/M	calculated-to-measured ratio
CSN	Consejo de Seguridad Nuclear
DOE	U.S. Department of Energy
DRC-ICPMS	ICPMS equipped with a dynamic reaction cell
EFPD	effective full-power day
ENDF/B	Evaluated Nuclear Data Files
ENUSA	Enusa Industrias Avanzadas, S.A.
EOB	end-of-burnup
GWd	gigawatt-day
HPLC	high performance liquid chromatography
ICPMS	inductively coupled plasma mass spectrometry
IDA	isotope dilution analysis
JEFF	Joint Evaluated Fission and Fusion File
LWR	light water reactor
MC-ICPMS	multicollector ICPMS
MALIBU	MOX and UOX LWR Fuels Irradiated to High Burnup
MOX	mixed oxide
MS	mass spectrometry
MTU	metric ton uranium (10^6 grams)
NRC	U.S. Nuclear Regulatory Commission
ORNL	Oak Ridge National Laboratory
PSI	Paul Scherrer Institute
PWR	pressurized water reactor
Q-ICPMS	quadrupole ICPMS
SCALE	a comprehensive modeling and simulation suite for nuclear safety analysis and design
SCK•CEN	Studiecentrum voor Kernenergie – Centre d'Étude de l'Energie Nucléaire
TIMS	thermal ionization mass spectrometry
UO$_2$	uranium dioxide
UOX	uranium oxide

1. INTRODUCTION

The current trend toward extended irradiation cycles and higher fuel enrichments of up to 5 wt % ^{235}U has led to an increase in the burnup range for discharged nuclear fuel assemblies. In addition, boiling water reactor (BWR) fuel assembly designs have become increasingly complex and heterogeneous compared to past designs, leading to improved performance. As the design and operating characteristics of BWR fuel have evolved dramatically, it is important that the computer codes and nuclear data used to simulate the lattice physics and nuclide compositions of spent nuclear fuel be validated using experimental data representative of modern assembly designs. The majority of isotopic assay measurements available for BWR fuel to date [1] involves burnups of less than about 40 GWd/MTU and early assembly designs that do not represent the complexity of the modern designs currently is use. In addition, measurements are largely available only for actinides, with limited fission product data. Thus, the present lack of representative data limits the ability to directly validate computer code predictions and accurately quantify the uncertainties in calculated nuclide compositions used in safety and licensing analyses of reactors and spent fuel storage facilities.

This report describes recently acquired radiochemical assay data that can be used to validate computer code predictions of the isotopic compositions in modern high burnup BWR fuel. The experimental data were acquired from two international programs:

- the MALIBU (Radiochemical Analysis of MOX and UOX LWR Fuels Irradiated to High Burnup) Extension program [2] coordinated by the Belgian research organization SCK•CEN (Studiecentrum voor Kernenergie – Centre d'Étude de l'Énergie Nucléaire), and
- a consortium of organizations in Spain, herein referred to as the ENUSA program, coordinated by the fuel manufacturer ENUSA (Enusa Industrias Avanzadas, S.A.), including the Spanish nuclear regulatory authority CSN (Consejo de Seguridad Nuclear) and the Spanish company responsible for radioactive waste management, ENRESA (La Empresa Nacional de Residuos Radiactivos, S.A.) [3].

The measurements available from the MALIBU Extension program include radiochemical assay data obtained from destructive analysis of three spent fuel samples selected from different axial elevations of a SVEA-96 Optima 10×10 assembly fuel rod, irradiated during seven reactor fuel cycles in the Swiss Leibstadt reactor. The ENUSA program provides data for six samples from a GE14 10×10 assembly fuel rod, irradiated during five fuel cycles in the Swedish Forsmark 3 reactor.

The radiochemical analysis measurements of the spent fuel samples were carried out at Studsvik Nuclear AB in Sweden, SCK•CEN in Belgium, and the Paul Scherrer Institute (PSI) in Switzerland. A summary of the experimental programs and measured fuel sample characteristics is listed in Table 1.1. The number of measured samples listed in the table reflects the unique samples. Several samples were measured independently at different laboratories.

The experimental data are used to validate the computational methods and nuclear data of the SCALE nuclear safety analysis code system [4] for the analysis of SVEA-96 Optima and GE14 10×10 assembly designs. The calculated isotopic contents in the spent fuel samples are compared to measurements for more than 60 nuclides important to a wide range of spent fuel applications including decay heat, radiation sources, and burnup credit criticality safety evaluations, as well as for reactor safety studies and accident consequence analyses.

At the time of the writing of this report, the experimental programs remain commercially restricted. Therefore, many of the details of the experimental program, including absolute measurement results, fuel design data, and reactor operating information, are not included in this report but will be published

separately at a later date when data will be made public. A brief description of the experimental programs is given in Section 2 of the report summarizing the radiochemical measurement methods employed and the associated experimental uncertainties. General information on the assembly design data and irradiation history is presented in Section 3, along with a description of the computational models developed for the simulation. Comparisons of the experimental data to the results obtained from code simulations are presented in Section 4.

Table 1-1. Summary of BWR spent fuel measurements

Reactor (country)	Measurement laboratory (country)	Experimental program	Assembly design	Enrichment (wt % ^{235}U)	No. of samples	Measurement methods[a]	Burnup(s)[b] (GWd/MTU)
Leibstadt (Switzerland)	Studsvik (Sweden), PSI (Switzerland), SCK•CEN (Belgium)	MALIBU Extension	SVEA-96 (10 × 10)	3.90	3	TIMS, ICPMS, MC-ICPMS, HPLC-ICPMS, α-spectrometry, γ-spectrometry	60.5, 62.9, 56.5
Forsmark 3 (Sweden)	Studsvik (Sweden)	ENUSA	GE14 (10 × 10)	3.95	6	ICPMS, HPLC-ICPMS, γ-spectrometry	38−52

[a] TIMS = thermal ionization mass spectrometry;
ICPMS = inductively coupled plasma mass spectrometry;
MC-ICPMS = multicollector ICPMS;
HPLC-ICPMS = high performance liquid chromatography with ICPMS.
[b] Values correspond to measured burnup as determined using ^{148}Nd.

2. EXPERIMENTAL PROGRAMS

This section provides a brief overview of the experimental isotopic assay data utilized in this report for code validation and a description of the international programs through which these data were acquired. A general description of the measurement techniques and uncertainties is also included.

2.1 MALIBU EXTENSION PROGRAM

The MALIBU experimental program [2], coordinated by SCK•CEN in Belgium, was initiated in 2003 to develop a database of high quality measurements of the isotopic content in irradiated nuclear fuel that can be used for code validation. The MALIBU program includes participants from laboratories and utilities from seven countries: Belgium, France, Germany, Japan, Switzerland, Sweden, and the United States. Oak Ridge National Laboratory (ORNL) has participated in the program through support of the U.S. Department of Energy and the U.S. Nuclear Regulatory Commission. The program provides extensive high-precision measurements for nuclides of importance to spent fuel source terms and burnup credit, and used three cross-checking laboratories for uncertainty quantification. The base program, completed in 2007, included measurements for high burnup commercial uranium oxide (UOX) and mixed oxide (MOX) fuels operated in pressurized water reactors (PWRs).

In 2007 the program was extended to include measurements of nuclide content for high burnup BWR UO_2 fuel. The laboratories participating in the extension program measurements included Studsvik Nuclear AB in Sweden, SCK•CEN in Belgium, and PSI in Switzerland. The spent fuel measurements were performed between 2009 and 2010, and include extensive actinide and fission product data of importance to spent fuel safety applications.

2.1.1 Leibstadt SVEA-96 Samples

The measured SVEA-96 fuel assembly AIA003 fabricated by Westinghouse Sweden was irradiated for seven consecutive cycles (cycles 15–21) in the Swiss Leibstadt reactor between August 21, 1998, and March 28, 2005. The general configuration of the SVEA-96 assembly design is illustrated in Figure 2-1.

All measurements were made for samples from fuel rod H6 (see Figure 2-1), with a nominal initial enrichment of 3.90 wt % ^{235}U and estimated rod-average burnup of 57.5 GWd/MTU. Rod H6 is internal to the assembly and thus relatively insensitive to changes in the surrounding assembly environment caused by movement of the assembly in the core during irradiation. However, rod H6 is also adjacent to an internal water cross of the assembly as well as a partial-length fuel rod and a rod containing gadolinium poison, thus providing a complex configuration for modeling.

Sections from three axial locations, referred to as KLU1, KLU2, and KLU3, were cut from rod H6 for radiochemical analysis.

- Sample KLU1 was obtained from the lower part of the fuel rod, where the void concentration is low and relatively stable.
- Sample KLU2 was obtained from the middle part of the fuel rod, where the void concentrations are higher and more variable.
- Sample KLU3 was obtained from a high elevation of the rod in the region where partial-length (short) fuel rods have "vanished" from the lattice and the void concentration is high and variable.
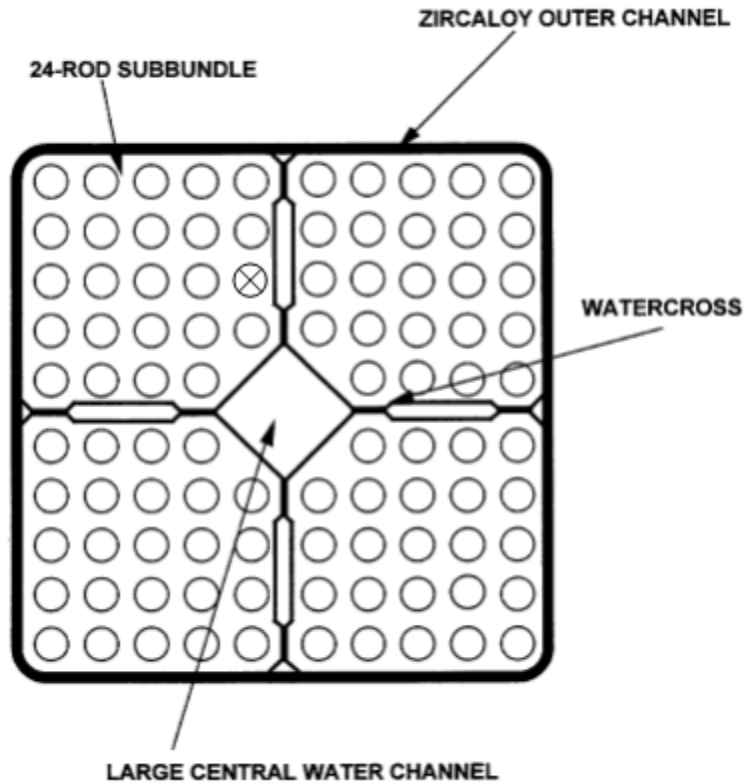
Figure 2-1. SVEA-96 fuel assembly cross section showing the location ⊗ of measured rod H6 (figure adapted from [5]).

Measurements of the KLU1 sample were performed at all three participating laboratories: Studsvik, SCK•CEN, and PSI. Note that Studsvik performed a second measurement of the KLU1 sample due to experimental problems that prevented measurement of some fission products in the first experiment. There were four adjacent samples from the selected fuel segment KLU1 samples in the fuel rod, which were used for the purpose of cross comparison of measurement data from the three laboratories. The KLU1 cross-check samples were designated as KLU1/1, KLU1/2, KLU1/3A, and KLU1/3B. Studsvik performed measurements on samples KLU1/1 and KLU1/3B. Only Studsvik performed measurements on samples KLU2 and KLU3. All these four cross-check samples have very similar burnups.

Table 2-1 provides a summary of sample identification names, the laboratories that carried out each analysis, and the axial location of the selected samples in the fuel rod. The reactor operating data is generated for 28 axial nodes. The axial node corresponding to the location of each sample is listed inTable 2-1. An axial gamma scan of the measured rod H6 is illustrated in Figure 2-2 showing the burnup profile and the location of the measured samples.

Table 2-1. Summary of SVEA-96 assembly AIA003 samples

Assembly and fuel rod ID	Fuel Segment ID	Burnup[a] (GWd/MTU)	Fuel Sample ID	Measurement laboratory	Sample elevation[b] (cm)	Sample axial node[c]	Sample assembly region[d]
AIA003-H6	KLU1	60.5	1	Studsvik	60.45–63.70	4	Dominant
			2	SCK•CEN	57.20–60.45	4	Dominant
			3A	PSI	56.10–57.20	4	Dominant
			3B	Studsvik	53.95–56.10	4	Dominant
AIA003-H6	KLU2	62.9	–	Studsvik	191.05–193.40	13	Dominant
AIA003-H6	KLU3	56.5	–	Studsvik	328.60–331.85	22	Vanished

[a] Burnup estimate based on measured ^{148}Nd content.
[b] Distance measured from the bottom of the fuel rod end plug.
[c] Axial node corresponding to the reactor operating data.
[d] Assembly region corresponding to locations below the top of the partial-length rods (dominant) and above the partial-length rods (vanished).
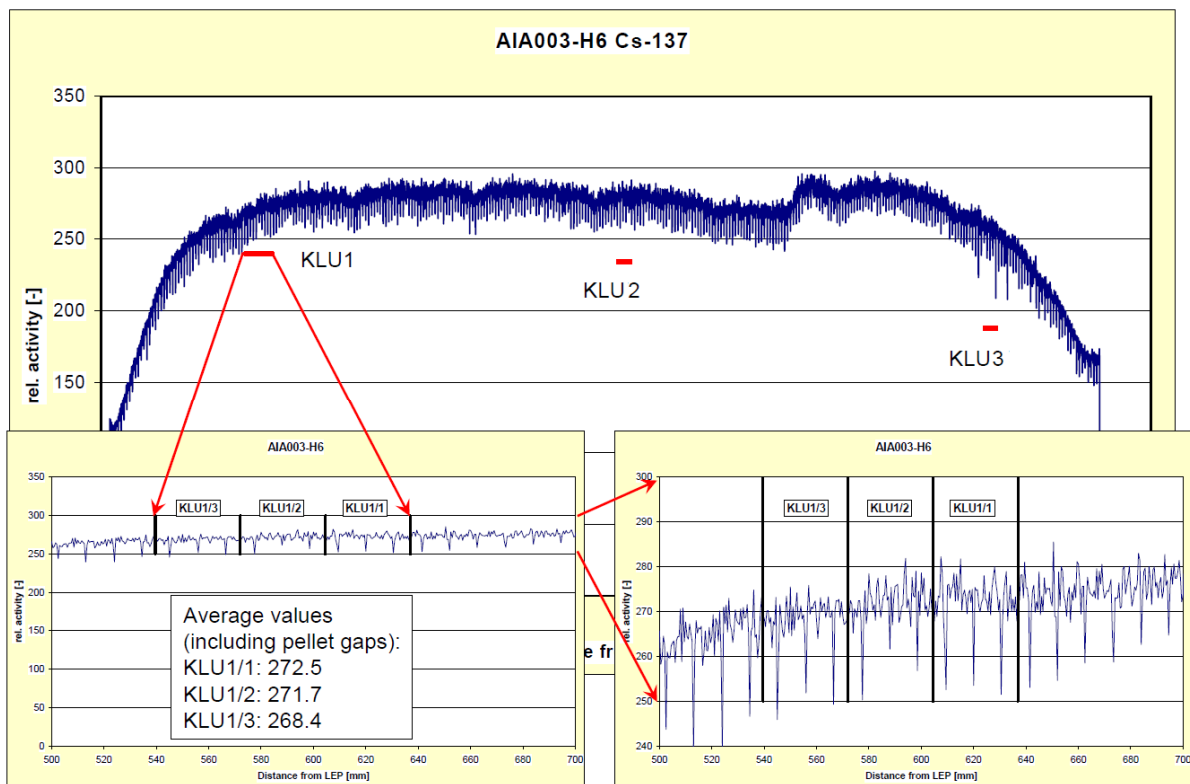
Figure 2-2. Axial gamma scan of measured fuel rod H6.

2.1.2 Measurements

Measurements of nuclide content performed by laboratories at Studsvik, SCK•CEN, and PSI included 53 isotopes (19 actinides and 34 fission products):

- uranium isotopes (234, 235, 236, 238)
- plutonium isotopes (238, 239, 240, 241, 242, 244)
- neptunium-237
- americium (241, 242m, 243)
- curium isotopes (242, 243, 244, 245, 246)
- cesium isotopes (133, 134, 135, 137)
- cerium-144
- neodymium isotopes (142, 143, 144, 145, 146 148, 150)
- promethium-147
- samarium isotopes (147, 148, 149, 150, 151, 152, 154)
- europium isotopes (151, 153, 154, 155)
- gadolinium-155
- strontium-90
- metallic nuclides (^{95}Mo, ^{99}Tc, ^{101}Ru, ^{106}Ru, ^{103}Rh, ^{109}Ag, ^{125}Sb)
- iodine-129

8

The main experimental techniques applied by Studsvik were high performance liquid chromatography with inductively coupled plasma mass spectrometry (HPLC-IDA-ICPMS). Isotope dilution analysis (IDA) was used for most nuclides for increased precision, with external calibration for other nuclides. In addition, α-spectrometry and γ-spectrometry measurement methods were used.

The experimental techniques applied by SCK•CEN included very high precision thermal ionization mass spectrometry (TIMS) with IDA for most nuclides, in addition to quadrupole inductively coupled plasma mass spectrometry (Q-ICPMS) with external calibration, and γ-spectrometry, α-spectrometry, and β-spectrometry.

The main experimental technique applied by PSI was HPLC and multi-collector inductively coupled plasma mass spectrometry (MC-ICPMS) with IDA for most nuclides. In addition, ICPMS with external calibration and γ-spectrometry were used.

Table 2-2 provides the details of the measured nuclides and the measurement method used by each laboratory for each nuclide. The measurement uncertainties estimated by the laboratories are listed and expressed at the 2σ (95%) confidence level. The metallic nuclides (^{90}Sr, ^{95}Mo, ^{99}Tc, ^{101}Ru, ^{106}Ru, ^{103}Rh, ^{109}Ag, ^{125}Sb) generally have larger measurement uncertainties. These nuclides are difficult to dissolve with standard dissolution techniques and generally require subsequent aggressive techniques to measure the undissolved fuel residues and obtain complete recovery. The estimated measurement uncertainties vary significantly between laboratories due to the use of different radiochemical analysis techniques and instruments. In general, the uncertainty of the Studsvik results are significantly larger than the uncertainties in the results reported by SCK•CEN and PSI.

The measurements were performed approximately five years after irradiation, and the analysis dates covered a period of several years. To obtain a consistent date for comparison of measurement results with calculations, the calculated results were decayed after irradiation to the measurement dates reported by each laboratory. Table 2-3 presents a summary of the measurement dates at each laboratory and the number of days post irradiation to the analysis date. The nuclides that require significant decay-time corrections are ^{240}Pu, ^{241}Pu, ^{241}Am, ^{242}Cm, ^{244}Cm, ^{134}Cs, ^{137}Cs, ^{144}Nd, ^{147}Sm, ^{154}Eu, ^{155}Eu, ^{154}Gd, and ^{155}Gd. The concentrations of several nuclides measured by gamma spectrometry were back-calculated to the time of discharge and reported as such by Studsvik.

Measurements performed at all laboratories included the separate analysis of undissolved residues. The metallic fission products, associated with the undissolved solids, were measured in the residues separately, and the residue content then added to the concentrations for the dissolved solution to obtain the total contents in the fuel sample.

A review of the laboratory cross-check measurements for sample KLU1 found the agreement of the SCK•CEN and PSI measurements were generally within the reported experimental uncertainties of several percent (see Table 2-2). However, systematic discrepancies were found between the nuclide content results reported by SCK•CEN and PSI and those reported by Studsvik. Notably, the Studsvik results for the plutonium isotopes were systematically 10–15% lower than those reported by the other two laboratories for the KLU1 sample. These deviations were observed in both KLU1 samples measured at Studsvik. The estimated 2σ uncertainty of the Studsvik plutonium measurements was approximately 3%. In addition, the uncertainties reported for the Studsvik measurements of neodymium isotopes (^{148}Nd used as the burnup indicator) were large, approximately 16% at the 95% confidence level, and the results showed similarly large systematic deviations in comparison with the other two laboratories. Based on the previous established performance of SCK•CEN and PSI in international measurement programs [2, 6], it is suspected that there were unidentified measurement problems at Studsvik.

At the time of writing of this report, the discrepancies in the measured nuclide concentrations, as reported by the laboratories, have not been resolved. Consequently, only the KLU1 measurements performed by SCK•CEN and PSI are considered in this report for code validation. The measurements for the samples measured by Studsvik (KLU1/1, KLU1/3B, KLU2, and KLU3) are not currently used but may be considered in the future if the cause of the suspected measurement issues is resolved.

Due to the current proprietary status of the MALIBU extension program, the measured nuclide contents are not included in this report. All benchmark results comparing calculations to the experiment are shown as relative concentrations.

Table 2-2. Experimental techniques and uncertainties for Leibstadt SVEA-96 samples

Nuclide	Measurements at Studsvik		Measurements at SCK•CEN		Measurements at PSI	
	Method[a]	Uncertainty[b] 2σ (%)	Method[a]	Uncertainty 2σ (%)	Method[a]	Uncertainty 2σ (%)
U-234	IDA-ICPMS	6.51	TIMS	0.79	IDA-HPLC-MC-ICPMS	0.59
U-235	IDA-ICPMS	3.38	TIMS	0.70	IDA-HPLC-MC-ICPMS	0.37
U-236	IDA-ICPMS	3.11	TIMS	0.69	IDA-HPLC-MC-ICPMS	0.36
U-238	IDA-ICPMS	2.01	TIMS	0.68	IDA-HPLC-MC-ICPMS	0.36
Pu-238	IDA-HPLC-ICPMS	5.89	TIMS	2.12	IDA-HPLC-MC-ICPMS	5.11
Pu-239	IDA-HPLC-ICPMS	3.15	TIMS	1.14	IDA-HPLC-MC-ICPMS	0.93
Pu-240	IDA-HPLC-ICPMS	3.26	TIMS	1.13	IDA-HPLC-MC-ICPMS	0.90
Pu-241	IDA-HPLC-ICPMS	3.48	TIMS	1.14	IDA-HPLC-MC-ICPMS	0.91
Pu-242	IDA-HPLC-ICPMS	3.55	TIMS	1.14	IDA-HPLC-MC-ICPMS	0.91
Pu-244	IDA-HPLC-ICPMS		TIMS	8.03	IDA-HPLC-MC-ICPMS	
Np-237	ICPMS	4.90	ICPMS	20.01	MC-ICPMS	5.00
Am-241	IDA-HPLC-ICPMS	4.87	TIMS	3.48	IDA-HPLC-MC-ICPMS	2.61
Am-242m			TIMS	34.60	IDA-HPLC-MC-ICPMS	20.17
Am-243	IDA-HPLC-ICPMS	5.75	TIMS	3.57	IDA-HPLC-MC-ICPMS	2.61
Cm-242	α-spec		α-spec	19.07		
Cm-243			γ-spec	14.61		
Cm-244	ICPMS	10.51	α-spec	14.61	IDA-HPLC-MC-ICPMS	18.01
Cm-245	ICPMS	11.66	TIMS	4.04	IDA-HPLC-MC-ICPMS	1.19
Cm-246	ICPMS	1.90	TIMS	10.02	IDA-HPLC-MC-ICPMS	1.23
Cs-133	IDA-HPLC-ICPMS	11.99	TIMS	6.23	IDA-HPLC-MC-ICPMS	1.50
Cs-134	IDA-HPLC-ICPMS	12.63	γ-spec	4.22	IDA-HPLC-MC-ICPMS	1.51
Cs-135	IDA-HPLC-ICPMS	11.98	TIMS	5.18	IDA-HPLC-MC-ICPMS	1.50
Cs-137	IDA-HPLC-ICPMS	11.96	γ-spec	4.09	IDA-HPLC-MC-ICPMS	1.50
Ce-144	γ-spec	18.84	γ-spec	6.27	IDA-HPLC-MC-ICPMS	15.49
Nd-142	IDA-HPLC-ICPMS	7.77	TIMS	1.69	IDA-HPLC-MC-ICPMS	0.68
Nd-143	IDA-HPLC-ICPMS	13.74	TIMS	1.68	IDA-HPLC-MC-ICPMS	0.11
Nd-144	IDA-HPLC-ICPMS	10.07	TIMS	1.67	IDA-HPLC-MC-ICPMS	0.11
Nd-145	IDA-HPLC-ICPMS	12.70	TIMS	1.67	IDA-HPLC-MC-ICPMS	0.35
Nd-146	IDA-HPLC-ICPMS	3.39	TIMS	1.68	IDA-HPLC-MC-ICPMS	0.26
Nd-148	IDA-HPLC-ICPMS	14.13	TIMS	1.83	IDA-HPLC-MC-ICPMS	0.46
Nd-150	IDA-HPLC-ICPMS	14.24	TIMS	2.38	IDA-HPLC-MC-ICPMS	0.57
Pm-147	IDA-HPLC-ICPMS	12.96	β-spec	27.36	IDA-HPLC-MC-ICPMS	11.32
Sm-147	IDA-HPLC-ICPMS	8.87	TIMS	1.08	IDA-HPLC-MC-ICPMS	0.97
Sm-148	IDA-HPLC-ICPMS	9.11	TIMS	1.08	IDA-HPLC-MC-ICPMS	0.97
Sm-149	IDA-HPLC-ICPMS		TIMS	1.09	IDA-HPLC-MC-ICPMS	23.22
Sm-150	IDA-HPLC-ICPMS	9.17	TIMS	1.08	IDA-HPLC-MC-ICPMS	0.97
Sm-151	IDA-HPLC-ICPMS	8.66	TIMS	1.10	IDA-HPLC-MC-ICPMS	1.01
Sm-152	IDA-HPLC-ICPMS	6.96	TIMS	1.07	IDA-HPLC-MC-ICPMS	0.99
Sm-154	IDA-HPLC-ICPMS	10.60	TIMS	1.09	IDA-HPLC-MC-ICPMS	1.05

Nuclide	Measurements at Studsvik		Measurements at SCK•CEN		Measurements at PSI	
	Method[a]	Uncertainty[b] 2σ (%)	Method[a]	Uncertainty 2σ (%)	Method[a]	Uncertainty 2σ (%)
Eu-151			TIMS	0.65	IDA-HPLC-MC-ICPMS	28.21
Eu-153	IDA-HPLC-ICPMS	15.75	TIMS	0.65	IDA-HPLC-MC-ICPMS	1.31
Eu-154	IDA-HPLC-ICPMS	17.24	TIMS	4.07	IDA-HPLC-MC-ICPMS	1.38
Eu-155	IDA-HPLC-ICPMS	26.22	TIMS	4.88	IDA-HPLC-MC-ICPMS	1.65
Gd-155	IDA-HPLC-ICPMS	28.12	TIMS	1.44	IDA-HPLC-MC-ICPMS	
Sr-90	DRC-ICPMS		β-spec	15.42	IDA-HPLC-MC-ICPMS	2.03
Mo-95	ICPMS	11.68	Q-ICPMS	15.01	MC-ICPMS	5.00
Tc-99	ICPMS	4.20	Q-ICPMS	15.01	MC-ICPMS	5.00
Ru-101	ICPMS	11.92	Q-ICPMS	15.01	MC-ICPMS	5.00
Ru-106	γ-spec	21.15	γ-spec	6.13	γ-spec	12.37
Rh-103	ICPMS	11.69	Q-ICPMS	15.01	MC-ICPMS	5.00
Ag-109	ICPMS	12.51	Q-ICPMS	15.01	MC-ICPMS	5.00
Sb-125	γ-spec	11.68	γ-spec	6.47	γ-spec	7.77
I-129			Q-ICPMS	40.39	γ-spec	6.60

[a] ICPMS, Inductively Coupled Plasma Mass Spectrometry with external calibration or separately determined response factors; IDA-ICPMS, Isotopic Dilution Analysis with ICPMS; IDA-HPLC-ICPMS, High Performance Liquid Chromatography with Isotopic Dilution Analysis and ICPMS; γ spec, gamma spectrometry; α-spec, alpha spectrometry; β-spec, beta spectrometry; MC-ICPMS, multicollector ICPMS with external calibration; Q-ICPMS, quadrupole ICPMS with external calibration; TIMS, Thermal Ionization Mass Spectrometry with Isotopic Dilution Analysis.
[b] Uncertainties for the Studsvik measurements are those reported for sample KLU1/1.

12

Table 2-3. Decay time data for Leibstadt SVEA-96 samples

Segment ID	KLU1								KLU2		KLU3	
Sample ID	KLU1/1		KLU1/2		KLU1/3A		KLU1/3B		KLU2		KLU3	
Measuring lab	Studsvik		SCK•CEN		PSI		Studsvik		Studsvik		Studsvik	
Nuclides	Measurement date (dd/mm/yy)	Decay time[a] (days)	Measurement date (dd/mm/yy)	Decay time[a] (days)	Measurement date (dd/mm/yy)	Decay time[a] (days)	Measurement date (dd/mm/yy)	Decay time[a] (days)	Measurement date (dd/mm/yy)	Decay time[a] (days)	Measurement date (dd/mm/yy)	Decay time[a] (days)
Uranium	30/06/10	1922	10/04/09	1467	12/03/10	1808	12/04/10	1843	12/04/10	1843	12/04/10	1843
Plutonium	28/04/10	1859	09/04/09	1466	20/03/10	1816	28/04/10	1859	28/04/10	1859	28/04/10	1859
Neptunium	03/02/10	1775	06/05/10	1864	01/09/10	1981	03/02/10	1775	03/02/10	1775	03/02/10	1775
Americium	28/04/10	1859	17/12/09	1724	22/10/10	2032	28/04/10	1859	28/04/10	1859	28/04/10	1859
Curium(242,243)	28/03/05	0	27/03/09	1459	22/10/10	2032	06/05/10	1867	06/05/10	1867		
Curium(244,245,246)	03/02/10	1775	17/12/09	1724	22/10/10	2032	06/05/10	1867	06/05/10	1867	03/02/10	1867
Neodymium	08/12/10	2083	26/06/09	1550	25/05/10	1882	08/12/10	2083	08/12/10	2083	08/12/10	2083
Iodine			01/10/09	1647	06/01/10	1743						
Cesium(133,135)	29/04/10	1860	23/03/09	1639	19/08/10	1968	29/04/10	1860	29/04/10	1860	29/04/10	1860
Cesium(134,137)	29/04/10	1860	26/03/09	1458	19/08/10	1968	29/04/10	1860	29/04/10	1860	29/04/10	1860
Cerium	28/03/05	0	26/03/09	1458	27/01/10	1764	28/03/05	0	28/02/05	0	28/03/05	0
Promethium	08/12/10	2083	13/08/09	1598	15/07/10	1933	08/12/10	2083	08/12/10	2083	08/12/10	2083
Samarium	08/12/10	2083	03/07/09	1557	15/07/10	1933	08/12/10	2083	08/12/10	2083	08/12/10	2083
Europium	08/12/10	2083	03/08/09	1588	19/07/10	1937	08/12/10	2083	08/12/10	2083	08/12/10	2083
Gadolinium	08/12/10	2083	24/09/09	1640	19/07/10	1937	08/12/10	2083	08/12/10	2083	08/12/10	2083
Strontium			10/08/09	1595	17/08/10	1966	04/05/10	1865				
95Mo			17/05/10	1875	01/09/10	1981	11/10/10	2025	03/02/10	1775	03/02/10	1775
99Tc			17/05/10	1875	01/09/10	1981	03/02/10	1775	03/02/10	1775	03/02/10	1775
101Ru			17/05/10	1875	01/09/10	1981	04/02/10	1776				
103Rh, 109Ag			17/05/10	1875	01/09/10	1981	11/10/10	2025				
106Ru, 125Sb			26/03/09	1458	27/01/10	1764	28/03/05	0	28/03/05	0	28/03/05	0

[a] Discharge date 28/03/05.
[b] Nuclides reported at discharge were measured after discharge and the concentrations adjusted by the laboratory.

2.2 ENUSA PROGRAM

The Spanish experimental program [3], coordinated by ENUSA, involves a number of organizations including the Spanish safety council for nuclear activities, CSN, and the organization responsible for waste management in Spain, ENRESA, with support provided under this project from the U.S. Nuclear Regulatory Commission. The program aims at providing isotopic composition data suitable for benchmarking codes and computational models used in reactor safety studies as well as for interim storage, transportation, and final disposal of spent nuclear fuel. Measurements include an extensive set of 68 nuclides.

2.2.1 Forsmark 3 GE14 Samples

Fuel samples of rod J8 from GE14 (10×10) fuel assembly GN592 were measured at hot cell laboratories of Studsvik Nuclear AB. The configuration of the GE14 assembly is shown in Figure 2-3. Measured fuel rod J8 was located at the periphery of the assembly, away from the control blade side of the assembly. The initial enrichment of all samples from rod J8 was 3.95 wt % ^{235}U. The fuel assembly was fabricated by ENUSA and irradiated in the Forsmark 3 reactor during five consecutive operating cycles (cycle 16–20) from July 24, 2000, to May 28, 2005. The measured fuel rod attained an estimated rod average burnup of 41 GWd/MTU and peak burnup of 56 GWd/MTU.

The locations of the samples were selected to provide wide representation of the axial void distribution. The ^{137}Cs gamma scan of rod J8, shown in Figure 2-4, illustrates the burnup profile and location of the selected fuel rod segments for radiochemical analysis. Samples were not obtained in the natural uranium regions at the top and bottom of the fuel rod (shown later in Figure 3-6). Table 2-4 provides a summary of sample identification names, the elevation of the samples along the fuel rod, and the axial node corresponding to the operating history data. The elevations are measured from the lower end plug of the fuel rod. The distance from the lower end plug to the start of the active fuel region is about 40 mm.

A total of eight fuel samples were selected from fuel rod J8. Samples 1 and 2, and samples 3 and 7, were selected from adjacent axial locations of the rod (see elevations in Table 2-4 and locations in Figure 3-6) to verify measurement repeatability and uncertainty. These replicate samples are expected to have very similar compositions.

2.2.2 Measurements

All measurements were performed by Studsvik Nuclear AB in 2010. The measurements include 68 nuclides (14 actinides and 54 fission products) and 21 elements for each analyzed sample. The measured isotopes were selected primarily on the basis of importance to reactor operations (eigenvalue), nuclear criticality safety using burnup credit, decay heat, and neutron and gamma ray sources. Measured isotopes include:

- uranium isotope (234, 235, 236, 238)
- plutonium isotopes (238, 239, 240, 241, 242)
- neptunium-237
- americium (241, 243)
- curium isotopes (244, 246)
- cesium isotopes (133, 134, 135, 137)
- cerium (140, 142, 144)
- lanthanum-139

- neodymium isotopes (142, 143, 144, 145, 146 148, 150)
- samarium isotopes (147, 148, 149, 150, 151, 152, 154)
- europium isotopes (153, 154, 155)
- gadolinium (154, 155, 156, 157, 158)
- molybdenum (92, 94, 95, 96, 97, 98, 100)
- strontium-90
- metallic nuclides (^{99}Tc, ^{101}Ru, ^{102}Ru, ^{104}Ru, ^{106}Ru, ^{103}Rh, ^{109}Ag, ^{125}Sb)
- palladium (105, 107, 108, 110)
- cadmium (111, 112, 114)
- iodine-129

High performance liquid chromatography combined with IDA and inductively coupled plasma mass spectrometry (IDA-HPLC-ICPMS), and ICPMS without chemical separation, were applied for the analysis of individual isotopes. Nuclides without any isobaric overlap were assessed by ICPMS with external calibration and with separately determined response factors. Iodine and strontium were analyzed using a dynamic reaction cell (DRC) in combination with ICPMS. Gamma-emitting nuclides were analyzed by gamma spectrometry.

In many cases results were reported for several measurement methods. Measurements made with the HPLC- IDA-ICPMS technique were generally used when available, as they typically have the smallest measurement uncertainties. Measurements made with other independent techniques generally had larger uncertainties and were used to provide cross checks on measurement consistency and uncertainty estimates. Table 2-5 presents a summary of the measured isotopes and the measurement method. The tabulated measurement uncertainties are 2σ (95% confidence level), listed for sample 6 as a representative example.

Mass spectroscopy results were reported at the time of analysis. Nuclides that exhibit concentration variations with decay time were also back-calculated to the end of burnup (discharge) for the isotopes ^{240}Pu, ^{241}Pu, ^{241}Am, ^{244}Cm, ^{134}Cs, ^{137}Cs, ^{144}Nd, ^{147}Sm, ^{154}Eu, ^{155}Eu, ^{154}Gd, and ^{155}Gd. As the procedure of back calculating concentrations introduces additional uncertainties, the measurement results used in this report were those corresponding to the measurement date. All calculations therefore decayed the nuclide concentrations to the time of measurement for each nuclide. Measurements based on gamma spectroscopy were back calculated by the laboratory to the time of discharge. Results at the time of measurement were not available.

Measurements of the metallic fission products have been corrected for the contribution from undissolved residues. These residues from dissolution of the fuel were analyzed separately and the results added to the results from the main fuel solution. In general, the fraction of undissolved material for most elements was small and did not contribute to significant uncertainties in the results. Contamination of samples with naturally occurring molybdenum was identified. Corrections to the measurements resulted in large errors for ^{94}Mo after subtracting the contribution from contamination, so the measured results for this isotope were not considered.
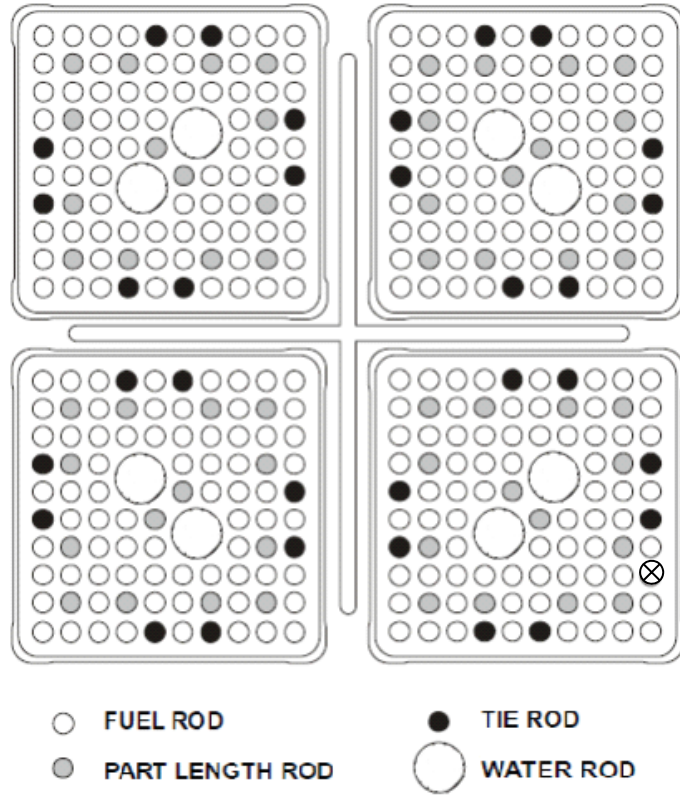
Figure 2-3. GE14 fuel assembly cross section and configuration, showing the location ⊗ of measured fuel rod J8 (figure adapted from [7]).
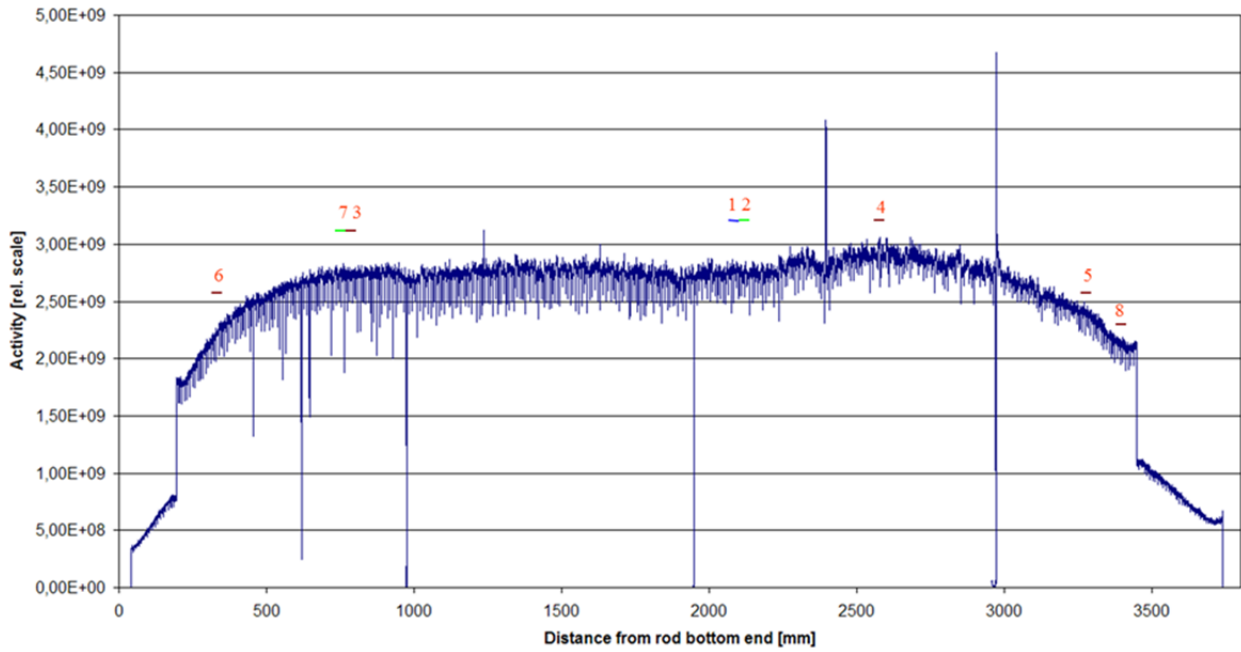
Figure 2-4. Gamma scan of the ^{137}Cs profile of rod J8 and locations of the measured samples.

Table 2-4. Summary of GE14 assembly GN592 samples

Assembly and fuel rod ID	Fuel sample ID	Sample burnup[a] (GWd/MTU)	Measurement laboratory	Sample elevation[b] (mm)	Sample axial node[c]	Sample assembly region[d]
GN592-J8	6	43.1	Studsvik Nuclear	397–407	3	Dominant
GN592-J8	7	47.8	Studsvik Nuclear	702–712	5	Dominant
GN592-J8	3	51.5	Studsvik Nuclear	712–722	5	Dominant
GN592-J8	1	50.4	Studsvik Nuclear	1842–1852	13	Dominant
GN592-J8	2	51.1	Studsvik Nuclear	1852–1862	13	Dominant
GN592-J8	4	56.0	Studsvik Nuclear	2503–2513	17	Vanished
GN592-J8	5	43.6	Studsvik Nuclear	3277–3287	22	Vanished
GN592-J8	8	38.3	Studsvik Nuclear	3384–3394	23	Vanished

[a] Burnup values reported by Studsvik based on destructive analysis of ^{148}Nd.
[b] Distance measured from the bottom of the fuel rod end plug.
[c] Axial node corresponding to the reactor operating data.
[d] Assembly region corresponding to locations below the top of the partial-length rods (dominant) and above the partial-length rods (vanished).

Table 2-5. Experimental techniques and typical uncertainties for Forsmark 3 GE14 samples

Nuclide	Method[a] (primary)	Uncertainty[b] 2σ (%)	Measurement date (dd/mm/yy)	Decay time[c] (days)
U-234	IDA-ICPMS	7.8	15/06/09	1540
U-235	IDA-ICPMS	3.1	15/06/09	1540
U-236	IDA-ICPMS	3.1	15/06/09	1540
U-238	IDA-ICPMS	2.0	15/06/09	1540
Pu-238	IDA-HPLC-ICPMS	4.1	16/06/09	1541
Pu-239	IDA-HPLC-ICPMS	3.0	16/06/09	1541
Pu-240	IDA-HPLC-ICPMS	3.2	16/06/09	1541
Pu-241	IDA-HPLC-ICPMS	2.8	16/06/09	1541
Pu-242	IDA-HPLC-ICPMS	4.0	16/06/09	1541
Np-237	ICPMS	12.6	25/05/09	1519
Am-241	IDA-HPLC-ICPMS	15.7	16/06/09	1541
Am-243	IDA-HPLC-ICPMS	23.1	16/06/09	1541
Cm-244	ICPMS	13.6	25/05/09	1519
Cm-246	ICPMS	87.5	25/05/09	1519
Cs-133	IDA-HPLC-ICPMS	2.9	31/08/09	1617
Cs-134	IDA-HPLC-ICPMS	1.5	31/08/09	1617
Cs-135	IDA-HPLC-ICPMS	2.8	31/08/09	1617
Cs-137	IDA-HPLC-ICPMS	2.2	31/08/09	1617
Ce-140	IDA-HPLC-ICPMS	6.5	01/07/09	1556
Ce-142	IDA-HPLC-ICPMS	3.4	01/07/09	1556
Ce-144	γ spec	16.9	28/03/05	0
La-139	ICPMS	12.3	25/05/09	1519
Nd-142	IDA-HPLC-ICPMS	5.0	01/07/09	1556
Nd-143	IDA-HPLC-ICPMS	4.3	01/07/09	1556
Nd-144	IDA-HPLC-ICPMS	3.6	01/07/09	1556
Nd-145	IDA-HPLC-ICPMS	5.2	01/07/09	1556
Nd-146	IDA-HPLC-ICPMS	3.0	01/07/09	1556
Nd-148	IDA-HPLC-ICPMS	7.4	01/07/09	1556
Nd-150	IDA-HPLC-ICPMS	5.0	01/07/09	1556

Table 2-5. (continued)

Nuclide	Method[a] (primary)	Uncertainty[b] 2σ (%)	Measurement date (dd/mm/yy)	Decay time[c] (days)
Sm-147	IDA-HPLC-ICPMS	12.6	01/07/09	1556
Sm-148	IDA-HPLC-ICPMS	10.2	01/07/09	1556
Sm-149	IDA-HPLC-ICPMS	35.3	01/07/09	1556
Sm-150	IDA-HPLC-ICPMS	10.4	01/07/09	1556
Sm-151	IDA-HPLC-ICPMS	28.6	01/07/09	1556
Sm-152	IDA-HPLC-ICPMS	9.7	01/07/09	1556
Sm-154	IDA-HPLC-ICPMS	12.5	01/07/09	1556
Eu-153	IDA-HPLC-ICPMS	5.9	01/07/09	1556
Eu-154	IDA-HPLC-ICPMS	4.8	01/07/09	1556
Eu-155	IDA-HPLC-ICPMS	8.9	01/07/09	1556
Gd-154	IDA-HPLC-ICPMS	11.1	01/07/09	1556
Gd-155	IDA-HPLC-ICPMS	14.6	01/07/09	1556
Gd-156	IDA-HPLC-ICPMS	9.8	01/07/09	1556
Gd-157	IDA-HPLC-ICPMS	30.0	01/07/09	1556
Gd-158	IDA-HPLC-ICPMS	11.1	01/07/09	1556
Mo-92	IDA-HPLC-ICPMS	41.0	28/10/09	1675
Mo-94	IDA-HPLC-ICPMS	48.5	28/10/09	1675
Mo-95	IDA-HPLC-ICPMS	42.8	28/10/09	1675
Mo-96	IDA-HPLC-ICPMS	66.7	28/10/09	1675
Mo-97	IDA-HPLC-ICPMS	42.7	28/10/09	1675
Mo-98	IDA-HPLC-ICPMS	42.7	28/10/09	1675
Mo-100	IDA-HPLC-ICPMS	42.8	28/10/09	1675
Sr-90	DRC-ICPMS[e]	11.6	08/09/09	1625
Tc-99	ICPMS	12.2	25/05/09	1519
Ru-101	ICPMS	12.2	25/05/09	1519
Ru-102	ICPMS	12.3	25/05/09	1519
Ru-104	ICPMS	12.3	25/05/09	1519
Ru-106	γ spec	17.8	28/03/05	0
Rh-103	ICPMS	12.2	25/05/09	1519
Pd-105	ICPMS	12.5	25/05/09	1519
Pd-107	ICPMS	12.1	25/05/09	1519
Pd-108	ICPMS	12.5	25/05/09	1519
Pd-110	ICPMS	12.8	25/05/09	1519
Ag-109	ICPMS	12.6	25/05/09	1519
Cd-111	ICPMS	16.0	25/05/09	1519
Cd-112	ICPMS	17.5	25/05/09	1519
Cd-114	ICPMS	19.3	25/05/09	1519
Sb-125	γ spec	16.1	28/03/05	0
I-129	DRC-ICPMS[e]	57.3	28/03/05	0

[a] ICPMS, Inductively Coupled Plasma Mass Spectrometry with external calibration or with separately determined response factors; IDA-HPLC-ICPMS, high performance liquid chromatography with Isotopic Dilution ICPMS; γ spec, gamma spectrometry; DRC-ICPMS, ICPMS equipped with a Dynamic Reaction Cell.
[b] Uncertainties listed are for sample 6.
[c] Discharge date March 28, 2005.

18

3. ASSEMBLY DESIGN AND MODELING DESCRIPTION

This section presents general information on the fuel assembly design, irradiation history, computational models, and methods. Details of the experimental program have not been publicly released at the time of the writing of this report. Therefore, a complete description of the design and operating history data are not included here and will be reported at a later date as additional information is made public.

3.1 COMPUTATIONAL METHODS AND NUCLEAR DATA

The computational modeling and simulation of the measurements was performed with TRITON, the two-dimensional (2-D) depletion sequence in the SCALE 6.1 computer code system [8]. TRITON couples the 2-D arbitrary polygonal mesh, discrete ordinates transport code NEWT with the depletion and decay code ORIGEN in order to perform the burnup simulation. At each depletion step, the transport flux solution from NEWT is used to generate cross sections and assembly power distributions for the ORIGEN calculations; the isotopic composition data resulting from ORIGEN is employed in the subsequent transport calculation to obtain cross sections and power distributions for the next depletion step in an iterative manner throughout the irradiation history.

All calculations employed the ENDF/B-VII 238-group cross-section library. Resonance self-shielding calculations were performed with the CENTRM module [9]. CENTRM prepares problem-dependent multigroup cross sections by performing a continuous-energy transport calculation in the resonance energy region using a cell representation of the fuel rods. The neutron flux solution from CENTRM is used by the PMC module to collapse point-wise cross sections to prepare the problem-dependent multigroup constants.

The collapsing option (`parm=weight`) in TRITON#was used to collapse the 238-group library to a problem-dependent 49-group library using the flux solution from an initial 238-group transport calculation. The collapsed 49-group library is used in all subsequent transport calculations during the depletion simulation. Default values were used for the convergence parameters in the transport calculation. Cross sections for all nuclides present in the ENDF/B-VII neutron transport libraries were applied in the ORIGEN depletion calculations (`addnux=4`). Cross sections for all other nuclides tracked by ORIGEN are obtained from collapsing 238-group cross sections developed from the JEFF-3.1/A special-purpose activation file with the 238-group flux determined from the NEWT neutron transport calculation. Time-dependent concentrations of approximately 2300 nuclides are tracked by ORIGEN. All nuclear decay data used in the ORIGEN depletion calculations are derived from ENDF/B-VII evaluations.

Individual models were developed for each of the measured samples discussed in the previous sections. The assembly geometry corresponding to either the dominant or vanished region of the assembly was determined from the axial height of each measured sample. The detailed power history was used in the simulations for each cycle as provided by the utility for each of the axial nodes. The irradiation history for each sample was normalized by adjusting the power to reproduce the measured concentration of [148]Nd in the sample within the experimental uncertainty (i.e., [148]Nd burnup). The model for each sample included the time-dependent variation of the moderator density and moderator temperatures provided by the utility.

Recent studies investigating the modeling and simulation of heterogeneous BWR assemblies using SCALE [10] identified several important findings that were applied in this study:

- The default Dancoff factors generated by TRITON for highly heterogeneous and high void lattices are not sufficiently accurate. These factors are calculated automatically from a simple cell

approximation and applied to the CENTRM resonance cross section self-shielding calculations. For fuel rods near the periphery of the assembly, the default Dancoff factors can be up to 30% different than values calculated with the explicit heterogeneous lattice geometry. To improve the Dancoff representation, externally calculated Dancoff factors from calculations using the 3-D Monte Carlo MCDancoff code [9] were included in the model for each fuel rod. MCDancoff is a modified version of the KENO-VI code used to compute Dancoff factors for arbitrary, nonuniform lattice configurations.

- Dancoff factors were first generated at 0%, 40%, 80%, and 100% void for the SVEA-96 and GE14 assembly designs. Because of the significant variation in the void between cycles, cycle-averaged values were interpolated and applied in each cycle simulation.

- To implement the externally calculated Dancoff factors for each cycle, it was necessary to model each cycle separately. The calculated fuel rod concentrations from the end of each cycle were applied as the initial concentration in the next cycle using a *boot-strap* approach that allows new cases to be restarted using compositions from a previous calculation.

- The irradiation history was simulated in detail with transport calculations performed at burnup intervals of approximately 2 GWd/MTU or less.

- The detailed time-dependent void history was applied in the calculations and updated at each transport calculation step using the `TIMETABLE` option in TRITON.

3.2 SVEA-96 OPTIMA ASSEMBLY

3.2.1 Description

SVEA-96 assembly AIA003 was irradiated in the Leibstadt reactor for seven consecutive cycles during cycles 15 to 21. The assembly was discharged March 28, 2005. The power levels, fuel temperatures, and void concentrations for each cycle were provided by the utility for the axial nodes corresponding to the sample locations. The data show large variations as functions of burnup in each of the three nodes that contained the measured fuel segments. [As examples, Figure 3-2 and Figure 3-3 show the variations of specific power level, fuel temperature, and void concentration in node 4 as a function of effective full-power days (EFPDs).]

The lattice configuration of the Leibstadt SVEA-96 Optima assembly AIA003 is shown in Figure 3-1. The presence of eight partial-length rods in the assembly results in different fuel rod configurations in the upper section (253.5 cm to 381.0 cm elevation) and lower section (0 cm to 253.5 cm elevation) of the assembly. The lower section of the assembly, with all fuel rods present, is referred to as the dominant zone. In the upper section, referred to as the vanished zone, the locations of the partial-length rods that contained fuel in the dominant zone are replaced by water. The measured H6 fuel rod, with an initial enrichment of 3.90 wt % ^{235}U, is highlighted in red. The axial locations of the samples from rod H6 are shown in

Figure 3-1. The axial nodes corresponding to the vanished zone are shown as shaded regions of the fuel rod. The figure illustrates the fuel rod configuration in the dominant and vanished zones of the assembly, and shows the fuel rod enrichment configuration (shown by unique rod number) and the locations of the U-Gd rods.

20
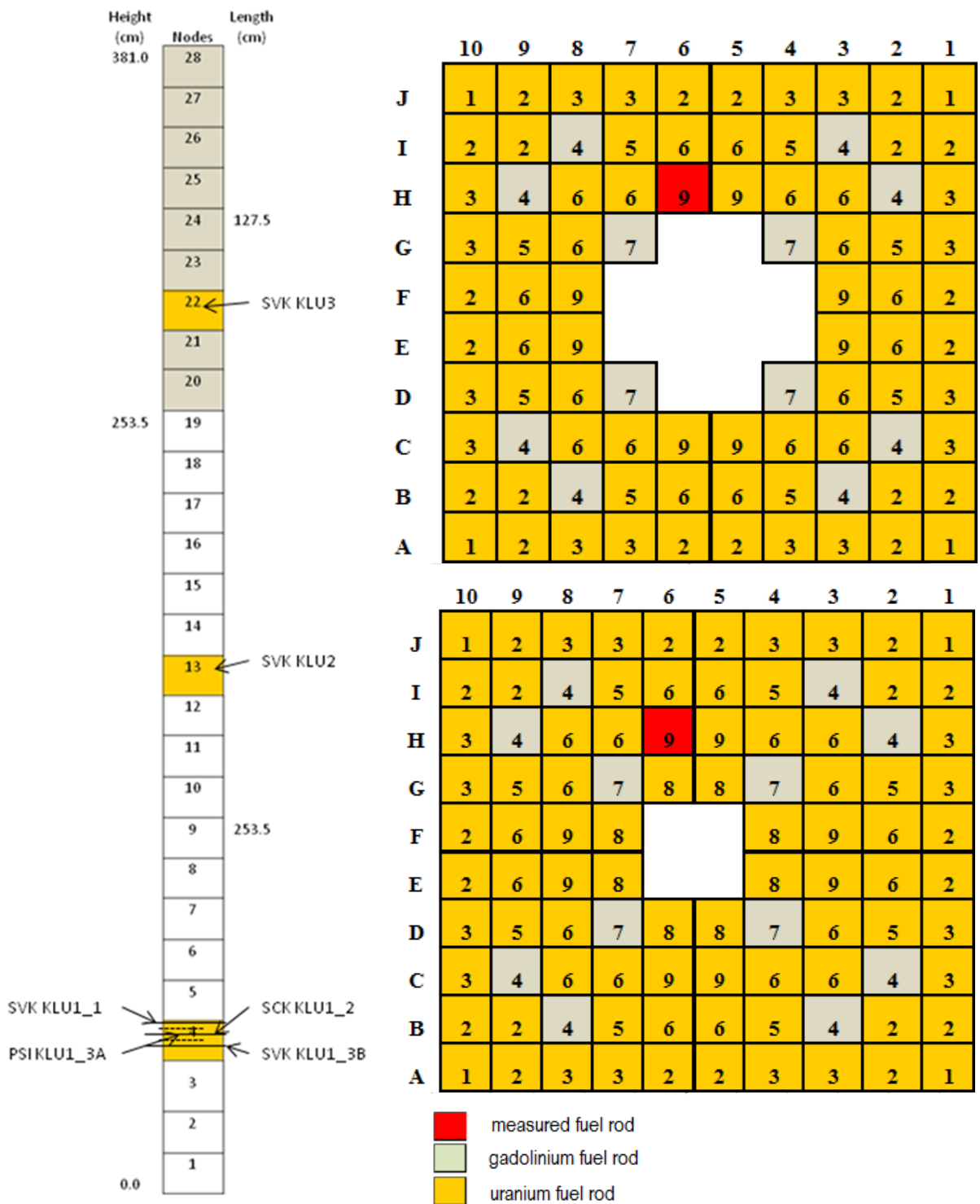
Figure 3-1. Leibstadt SVEA-96 assembly layouts for dominant zone (bottom) and vanished zone (top) and axial location of measured samples.
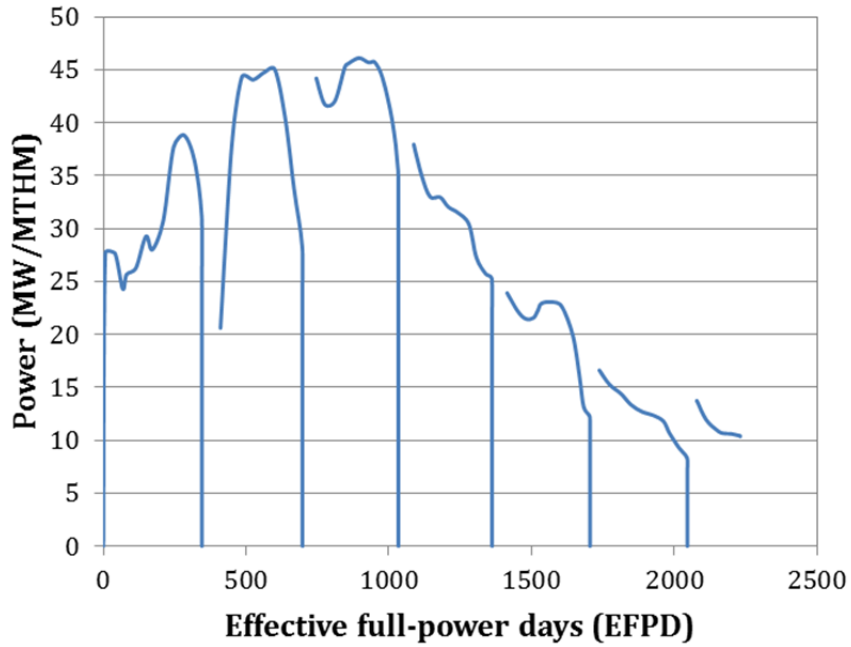
Figure 3-2. Power history for Leibstadt SVEA-96 assembly node 4.
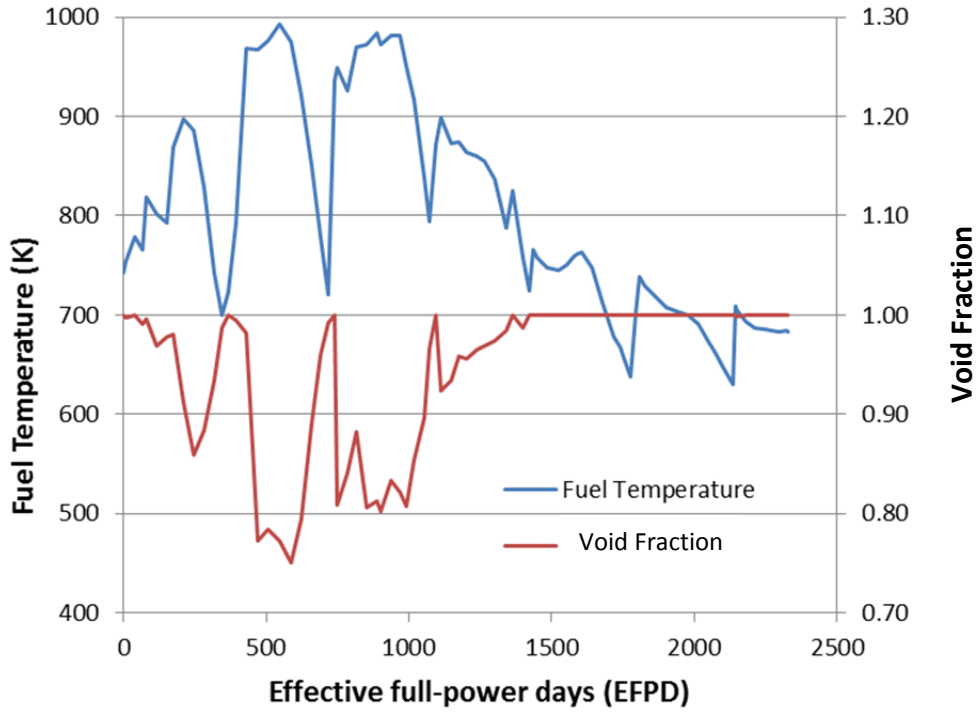
Figure 3-3. Fuel temperature and void histories for Leibstadt SVEA-96 assembly node 4.

Four samples from fuel segment KLU1 were obtained from adjacent elevations in node 4 of the dominant zone. Due to the small height of the KLU1 segment (3.25 cm), the fuel samples are expected to have experienced very similar operating conditions and have comparable isotopic compositions. These samples serve to monitor the repeatability of the measurements for uncertainty confirmation. Sample KLU2 was also taken from the dominant zone, while KLU3 was taken from the vanished zone. Sample KLU1 was measured by SCK•CEN, PSI, and Studsvik. Samples KLU2 and KLU3 were measured only by Studsvik. As discussed in Section 2, the Studsvik results were not used in this report. Therefore, only the KLU1 sample has been analyzed at this time.

3.2.2 Assembly Model

The Leibstadt SVEA-96 assembly AIA003 was analyzed with a quarter assembly model as shown in Figure 3-4 for the dominant zone (full lattice) and the vanished zone (lattice minus the partial-length rods). In this report, only the dominant zone model was used since KLU1 was the only sample analyzed in this study. All fuel rods were depleted individually, and radial subdivision of the gadolinium rods was used for more accurate time-dependent poison depletion. The enrichment zoning and location of the gadolinium rods in relation to the measured fuel rod is illustrated in Figure 3-1.

The irradiation history for sample KLU1 was developed from the operator-provided data for axial node 4 corresponding to the axial elevation of the sample. The detailed time-dependent information for node 4 provided by the utility included:

- thermal power history
- void history
- temperature history
- moderator history

These data were included in the model using the TIMETABLE option. As described previously, the Dancoff factors for each fuel rod were calculated externally and supplied to replace the default values that have been found to be inadequate for highly heterogeneous and high void lattices.

The calculated thermal flux distribution in the assembly (quarter assembly model) is illustrated in Figure 3-5.
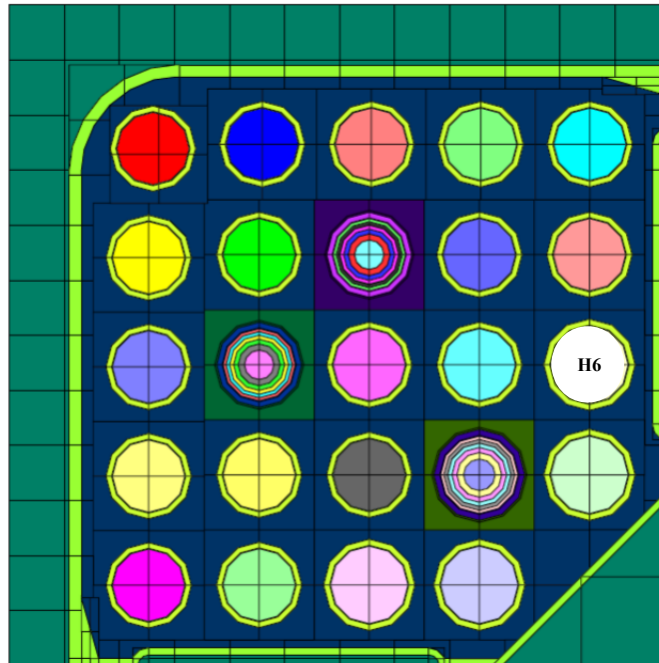
Figure 3-4. Subassembly (1/4) model for SVEA-96 dominant zone (bottom) and vanished zone (top).
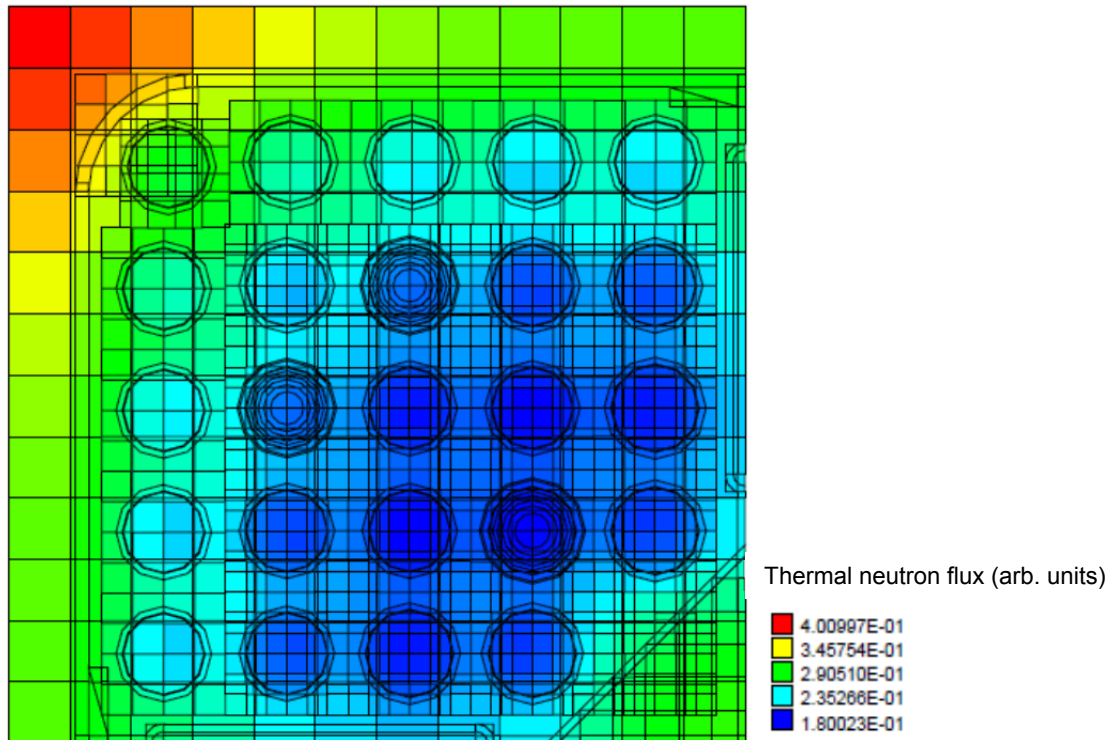
Figure 3-5. Thermal flux spatial distribution in subassembly model for SVEA-96 dominant zone.

3.3 GE14 ASSEMBLY

3.3.1 Description

The fuel rod configuration of GE14 assembly GN592 is shown in Figure 3-6 for the lower section dominant zone (unshaded length of rod from 0 cm to 220.8 cm elevation) and upper section vanished zone (shaded length of the fuel rod from 220.8 cm to 368.0 cm). In the vanished zone, the locations of the 14 partial-length rods that contained fuel in the dominant zone are replaced by water. The assembly design is highly heterogeneous, with nine different fuel enrichments and partial-length rods.

The location of measured fuel rod J8 in Figure 3-6 is highlighted in red. This rod had an initial enrichment of 3.95 wt % and is positioned at the edge of the assembly, with an adjacent U-Gd rod and partial-length rod with water-filled adjacent site in the vanished region of the assembly. The axial location of the eight samples from rod J8 are also shown in Figure 3-6. The green-shaded regions at the top and bottom sections of the rod contain natural uranium. Samples 1, 2, 3, 6, and 7 were all obtained from the dominant zone. Samples 1 and 2 are taken from adjacent locations in axial node 13, and samples 3 and 7 are from adjacent locations in node 5. Due to the small axial length of the samples (1.0 cm), significant differences in operating conditions and isotopic composition of the fuel between adjacent samples are not expected, and these samples serve to verify the repeatability of the measurements for uncertainty confirmation. Samples 4, 5, and 8 were taken from the vanished region.

25

Figure 3-7 illustrates the variation of specific power level and moderator void concentration in node 5 as a function of effective full-power days (EFPD) during cycles 16 to 20. Figure 3-8 shows the specific power and void for node 23, located near the top of the assembly. The power level and moderator void exhibit large variations during irradiation in each of the six nodes that contained the measured fuel segments. These variations were explicitly modeled. Only the average fuel temperature was provided by the reactor operator.
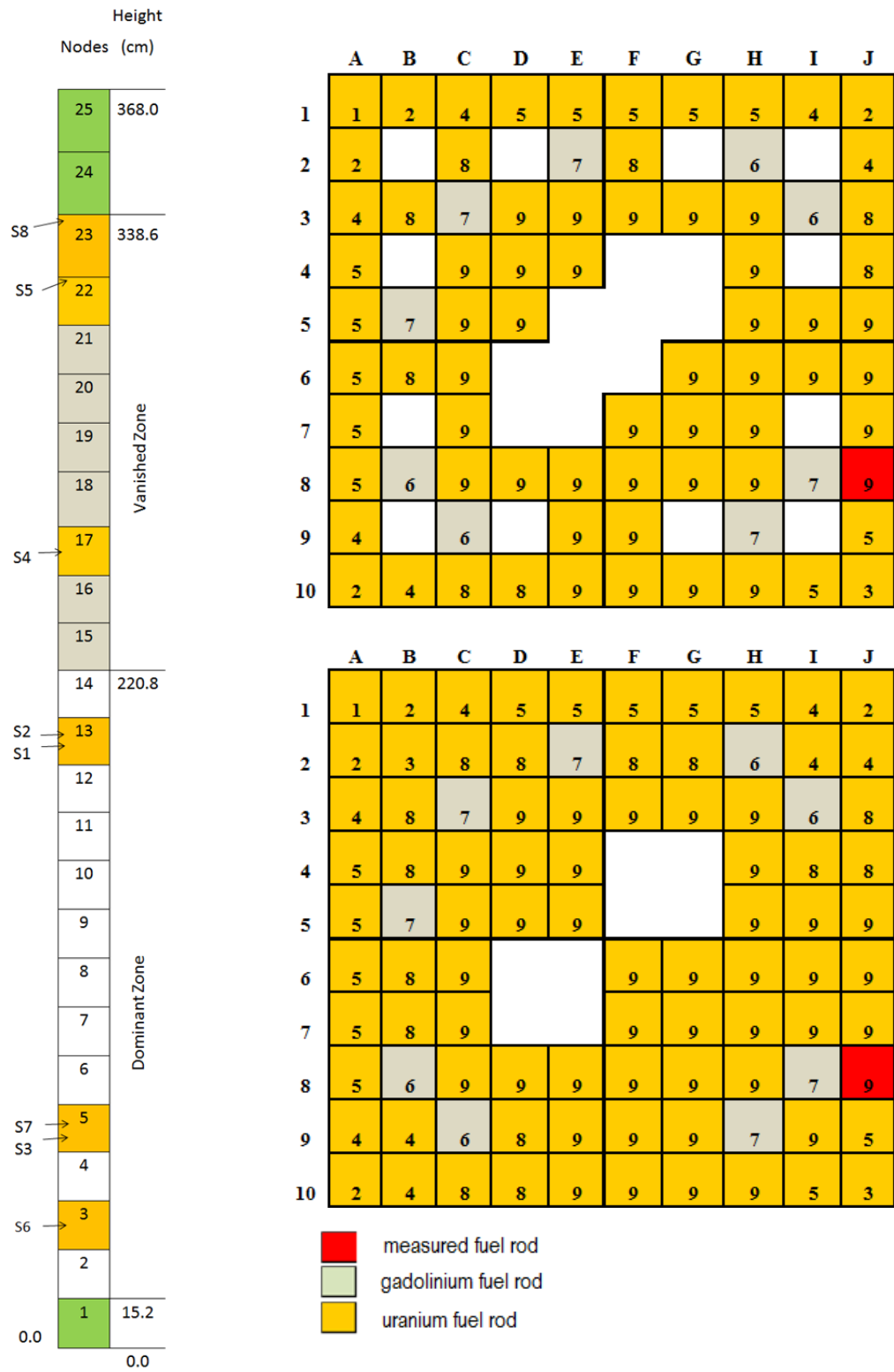
Figure 3-6. GE14 assembly layout showing fuel rod configuration for dominant zone (bottom) and vanished zone (top), and axial locations of measured samples in rod J8.

27
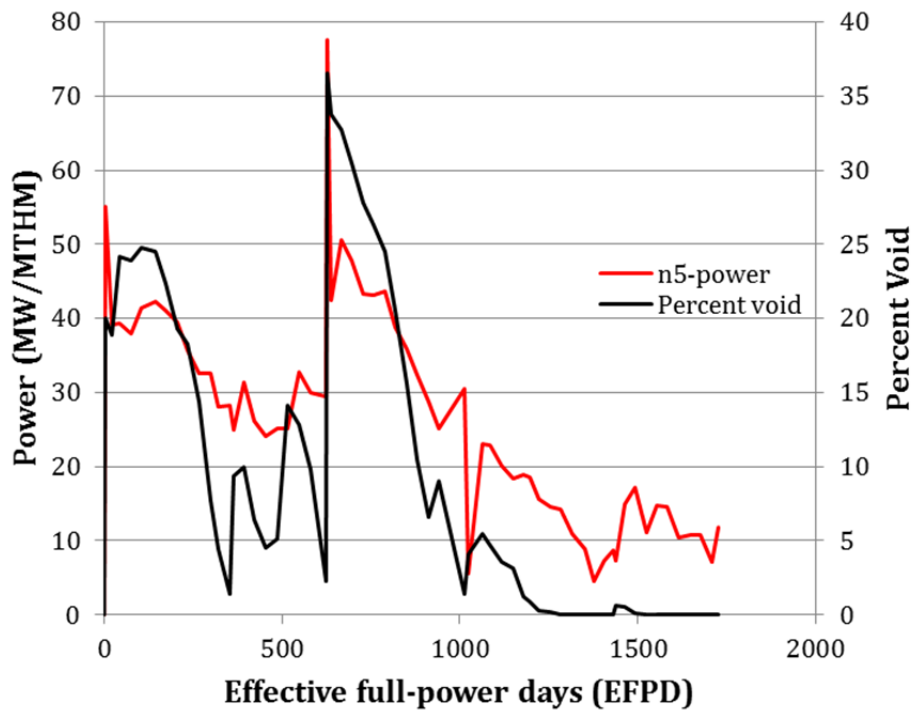
Figure 3-7. Power and moderator void histories for Forsmark 3 GE14 node 5.
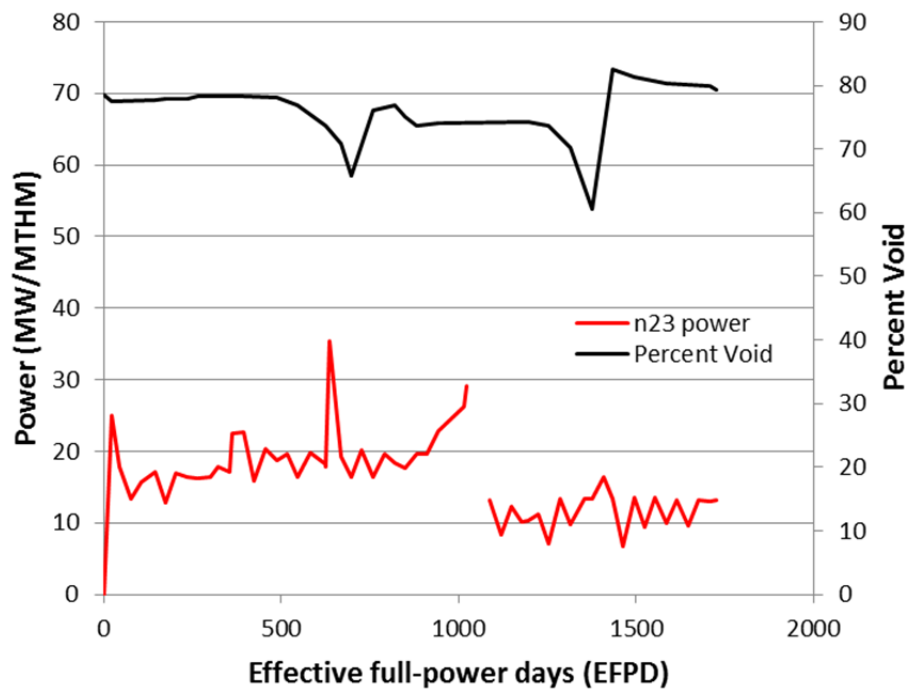
Figure 3-8. Power and moderator void histories for Forsmark 3 GE14 node 23.

3.3.2 GE14 Assembly Model

The geometry of the GE14 10×10 assembly GN592 was modeled in full detail because there is only twofold symmetry in the assembly with respect to the placement of the gadolinium-bearing U-Gd rods. Figure 3-9 shows the dominant and vanished-zone lattice models. Radial subdivision of the gadolinium rods was used for more accurate time-dependent poison depletion.

Because rod J8 was located on a narrow-gap side at the periphery of the assembly, away from the control blade, the control blade was not included in the model. Information on the neighbor assemblies during each cycle was provided by the utility. In this study, the neighbors were not included in the model and a white boundary condition was used for the assembly bounding conditions, simulating an infinite array of like assemblies. The relatively large separation of the assemblies (compared to PWR assemblies) is considered to significantly reduce the degree of neutronic interaction and impact of the assembly neighbors on the measured fuel rod. Additional studies are under way to quantify the importance of including explicit neighbor assembly modeling on calculated spent fuel nuclide compositions.

The calculated thermal flux distribution in the full-assembly model is illustrated in Figure 3-10.
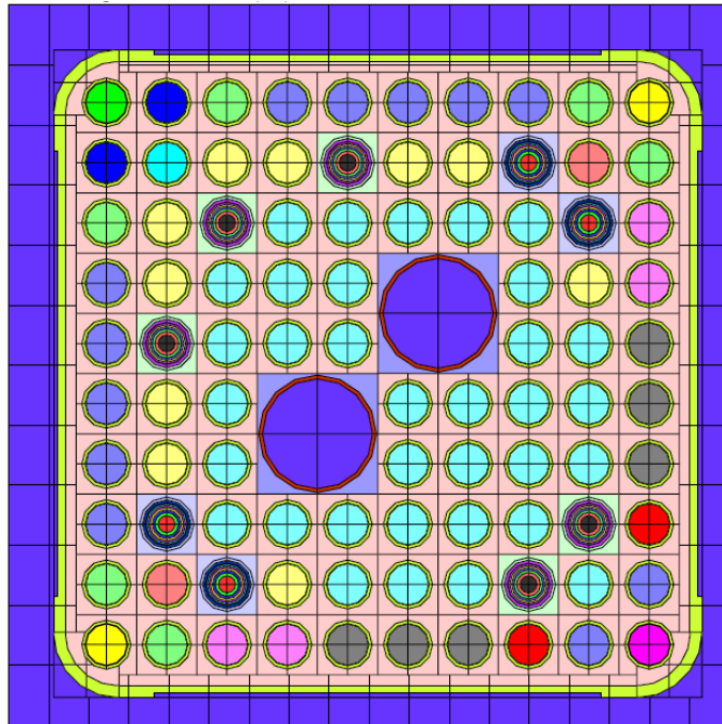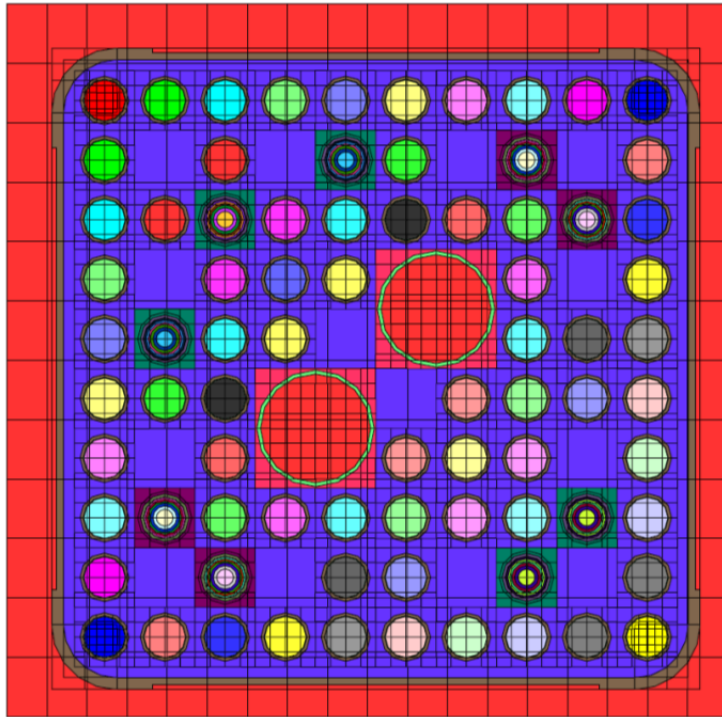
Figure 3-9. Full assembly model for GE14 dominant (bottom) and vanished zones (top).
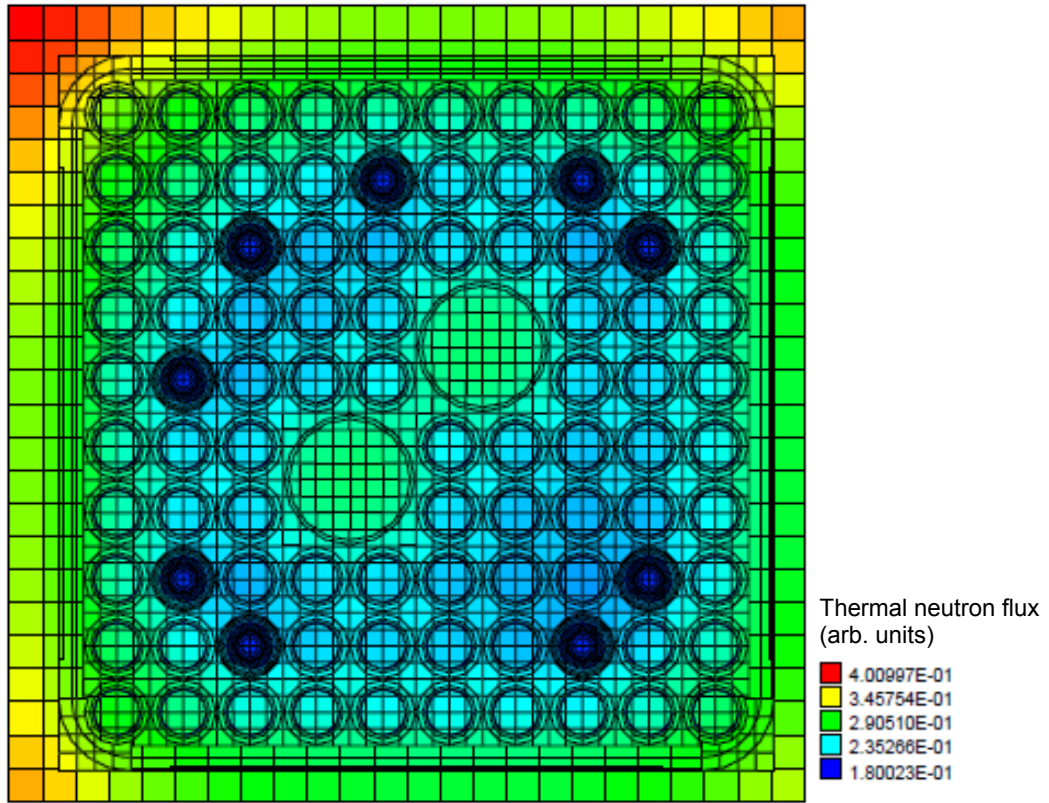
Figure 3-10. Thermal flux spatial distribution in full-assembly model for GE14 dominant zone.

4. RESULTS

This section presents comparisons of calculated isotopic concentrations for all spent fuel samples with concentrations determined experimentally. The deviations are expressed as percent difference between the calculated and measured concentrations, that is, $(C/M - 1) \times 100$, where M is the measured concentration of the isotope at the time of measurement and C is the calculated isotopic concentration at the decay time that corresponds to the reported measurement date.

The comparisons also include error bars associated with uncertainties in the measurements. The uncertainties evaluated in this report come from two sources: 1) a direct uncertainty associated with the nuclide measurements as reported by the measurement laboratory, and 2) an indirect uncertainty associated with uncertainty in the sample burnup, which is related to the uncertainty in the experimentally measured burnup monitors (e.g., ^{148}Nd and ^{137}Cs). The uncertainty due to burnup for a specific nuclide is estimated in this study on the basis of the measurement uncertainty for the measured burnup monitor and the sensitivity of that nuclide to changes in burnup. The sensitivity for each nuclide is determined by using calculated concentrations near the time of discharge. The burnup uncertainty is therefore different for each sample and each nuclide. The two components of measurement uncertainty provide a more realistic estimate of the total uncertainty. The total uncertainty for each isotope was estimated by combining measurement uncertainties (σ_M) and burnup uncertainty (σ_B) as

$$\sigma_T = \sqrt{\sigma_M^2 + \sigma_B^2} \qquad (1)$$

with the exception of the measurement of the burnup indicator, as these uncertainty components are largely uncorrelated.

The results are tabulated for each sample and measured nuclide as:

- the percent deviation of the calculated concentration compared with the measured value $(C/M - 1)$,
- reported 2σ measurement uncertainties,
- the uncertainty associated with the measured burnup for the sample (determined from the measured ^{148}Nd burnup value at the 95% uncertainty limit) and the nuclide sensitivity to burnup, and
- the total uncertainty combining both the measured and burnup uncertainty contributions σ_T in Eq. (1).

Neodymium-148 is widely used as a fission product for burnup estimation. In the case of the Studsvik measurement of the GE14 fuel samples in the ENUSA program, the ^{148}Nd measurement uncertainty (95% confidence) was relatively large, ranging from about 4% to 14%. For samples with large ^{148}Nd measurement uncertainty, additional burnup monitors with generally much smaller measurement uncertainties were considered for burnup confirmation, including ^{137}Cs, ^{139}La, and ^{148}Nd. In these cases however, the burnup uncertainty is still represented by the measured ^{148}Nd uncertainty, resulting in a likely overestimation of the total measurement uncertainty for these samples.

4.1 LEIBSTADT SVEA-96 SAMPLES

4.1.1 KLU1

Sample KLU1 was obtained from fuel rod H6 of Leibstadt assembly AIA003. As discussed previously, only the KLU1 sample is currently considered for use in code validation due to suspected problems associated with the Studsvik measurements of the KLU2 and KLU3 samples at the present time. The KLU1 measurements used in this report were those performed independently by SCK•CEN and PSI.

The uncertainties associated with the KLU1 sample burnup are very small due to the very high precision of measurements performed on the TIMS and MC-ICPMS instruments at SCK•CEN and PSI, respectively (1.8% and 0.5% uncertainty in ^{148}Nd at the 95% confidence level).The ^{148}Nd contents measured by the two laboratories, used for burnup determination, were in good agreement, within 2.6%. As the KLU1 samples are duplicates with the same expected nuclide content, a single calculation was performed. The ^{148}Nd burnup value used in the calculations was the value determined by PSI. This value had a smaller measurement uncertainty and yielded consistent agreement between calculated values for ^{137}Cs and ^{90}Sr (alternative burnup indicator fission products) and measured results from both laboratories.

Table 4-1 presents the results for the actinides and fission products of the KLU1 sample against both the SCK•CEN and PSI measurements. Because the measurements from both laboratories are compared to results from the same calculation, the deviations between the two sets of laboratory results reflect the differences between the measurements for the sample.

Figure 4-1 shows the results for actinides, and fission product isotopes of cesium, cerium, and neodymium. Figure 4-2 shows results for the isotopes of samarium, europium, the metallic nuclides, and several radiologically important isotopes. A constant scale has been used on the *y*-axis (% deviation) in these figures to preserve the relative magnitude of the deviations.

The agreement between the independent measurements performed by SCK•CEN and PSI is extremely good, and most measurements agree within the estimated experimental uncertainties. The largest differences observed between laboratories are several isotopes of americium and curium, ^{144}Ce, and the metallic fission products.

The calculated results for the major uranium and plutonium isotopes are observed to be in good agreement with measurements. These isotopes generally agree to better than 6.5% with the notable exception of ^{238}Pu, underpredicted by ~12%. The measured results for ^{235}U are consistent between the two laboratories (3% difference), although the observed differences between calculations and measurements are larger than the estimated measurement uncertainties at both laboratories (<1% at the 95% confidence level). A similar difference is observed for ^{239}Pu. Some differences may be attributed to axial variations in the nuclide content of the two samples caused by local variations in the sample environment, although the close proximity of the samples, cut from adjacent positions of the fuel rod, suggests nearly identical compositions as has been assumed in this report (i.e., separate calculations were not performed for each sample).

The results for the minor actinides show more variability than the major actinides. Note that these nuclides also have much larger measurement uncertainty. The curium isotopes exhibit significant differences between laboratories, indicating a significant level of uncertainty in the measurement data.

Cesium isotopes (important decay heat and radiological nuclides) are in good agreement with measurements, within < 6%, with the exception of ^{134}Cs, which is overpredicted by ~10%. The result for

[134]Cs is notably different than the one observed in a recent isotopic validation study for PWR fuel samples [11] that showed good agreement of measurements with calculations performed using ENDF/B-VII cross sections. The concentration of ^{134}Cs is very sensitive to the ^{133}Cs neutron capture cross section (significant changes in calculated results were observed when changing from ENDF/B-V to ENDF/B-VII cross sections for PWR fuel analysis). The consistent laboratory results for all cesium isotopes considered here suggests a possible deficiency in the model, possibly related to the cross sections for heterogeneous lattices with high moderator void.

Neodymium isotopes are predicted within 6.8% of the measurements. The samarium isotopes show a consistent level of agreement, also within 6.7%. The laboratory measurements of the europium isotopes are consistent and show an underprediction of ^{151}Eu and overprediction of the important gamma-emitting nuclide ^{154}Eu. The laboratory results for ^{155}Eu and ^{155}Gd are inconsistent, indicating potential measurement problems. The deviations between calculations and measurements for ^{155}Eu and ^{155}Gd are expected to be very similar because the concentration of ^{155}Gd is produced entirely from the decay of ^{155}Eu after discharge. Therefore any bias in ^{155}Eu will directly impact ^{155}Gd bias with a similar magnitude. These deviations are not consistent, again, possibly indicating biases in the measurements or errors in the decay times used in the calculations.

The calculated result for ^{90}Sr, an important radiological beta emitter and contributor to dose in safety analyses, is in excellent agreement with measurements, within 1.3%. The results for ^{129}I, another important radionuclide for long-term waste management safety studies, show that this nuclide is predicted within 19% of the measurements, although there is considerable uncertainty in the measurements.

The metallic nuclides ^{95}Mo, ^{99}Tc, ^{109}Ag, and ^{103}Rh have large neutron capture cross sections and are important in nuclear criticality safety (burnup credit). The results between the different laboratories are in fair agreement and suggest the calculated concentrations are generally overpredicted. These nuclides are difficult to measure because they are insoluble in nitric acid, and measurements frequently underestimate the content due to incomplete recovery of the nuclides into solution. However, the level of agreement between the independent laboratory measurements indicates that the observed discrepancy is more likely attributed to calculations than to measurements.

Table 4-1. Results for Leibstadt SVEA-96 sample KLU1

Sample ID	KLU1/2				KLU1/3A			
Measuring lab	SCK•CEN				PSI			
		2σ uncertainties				2σ uncertainties		
Nuclide	C/M-1 (%)	Meas. (%)	Burnup (%)	Total (%)	C/M-1 (%)	Meas. (%)	Burnup (%)	Total (%)
U-234	2.8	0.8	0.5	0.9	0.7	0.7	0.5	0.9
U-235	6.6	0.7	2.4	2.5	3.4	0.4	2.4	2.4
U-236	-2.4	0.7	0.0	0.7	-3.7	0.4	0.0	0.4
U-238	0.2	0.7	0.0	0.7	-1.2	0.4	0.0	0.4
Pu-238	-11.0	2.1	0.9	2.3	-12.0	5.1	0.9	5.2
Pu-239	7.5	1.1	0.2	1.2	4.3	0.9	0.2	0.9
Pu-240	3.3	1.1	0.2	1.1	1.0	0.9	0.2	0.9
Pu-241	3.5	1.1	0.0	1.1	2.3	0.9	0.0	0.9
Pu-242	-6.2	1.1	0.9	1.5	-7.5	0.9	0.9	1.3
Np-237	6.7	20.0	0.4	20.0	14.1	5.0	0.4	5.0
Am-241	19.7	3.5	1.0	3.6	4.5	2.6	1.0	2.8
Am-242m	-18.2	34.6	1.4	34.6	-12.6	20.2	1.4	20.2
Am-243	8.0	3.6	1.3	3.8	7.6	2.6	1.3	2.9
Cm-242	-18.7	19.1	1.7	19.1				
Cm-243	-28.5	14.6	0.4	14.6	108.9	18.0	0.4	18.0
Cm-244	-6.0	14.6	1.8	14.7	-17.4	1.2	1.8	2.2
Cm-245	27.9	4.0	2.0	4.5	-1.6	1.2	2.0	2.4
Cm-246	48.4	10.0	3.3	10.5	-26.5	1.2	3.3	3.5
Cs-133	6.3	6.2	0.3	6.2	2.0	1.5	0.3	1.5
Cs-134	9.4	4.2	0.1	4.2	11.0	1.5	0.1	1.5
Cs-135	2.7	5.2	0.7	5.2	1.0	1.5	0.7	1.7
Cs-137	-0.5	4.1	0.4	4.1	0.1	1.5	0.4	1.5
Ce-144	13.1	6.3	2.0	6.6	-11.4	15.5	2.0	15.6
Nd-142	-0.4	1.7	1.3	2.1	-0.6	0.8	1.3	1.5
Nd-143	6.8	1.7	0.2	1.7	4.7	0.2	0.2	0.3
Nd-144	-1.0	1.7	0.8	1.8	-2.4	0.2	0.8	0.8
Nd-145	-0.5	1.7	0.3	1.7	-2.5	0.4	0.3	0.5
Nd-146	2.5	1.7	0.6	1.8	0.9	0.3	0.6	0.7
Nd-148	2.6	1.8	0.5	1.9	0.2	0.5	0.5	0.7
Nd-150	3.7	2.4	0.5	2.4	0.9	0.6	0.5	0.8
Pm-147	6.2	27.4	0.9	27.4	17.9	11.3	0.9	11.4
Sm-147	3.9	1.1	0.9	1.4	1.0	1.0	0.9	1.3
Sm-148	-1.8	1.1	0.9	1.4	-3.3	1.0	0.9	1.3
Sm-149	-3.8	1.1	0.4	1.2	-6.6	23.2	0.4	23.2
Sm-150	6.7	1.1	0.3	1.1	4.6	1.0	0.3	1.0
Sm-151	2.6	1.1	0.0	1.1	1.6	1.0	0.0	1.0
Sm-152	1.3	1.1	0.3	1.1	-0.8	1.0	0.3	1.0
Sm-154	3.4	1.1	0.6	1.3	5.0	1.0	0.6	1.2
Eu-151	-28.2	0.7	1.1	1.3	-27.4	28.2	1.1	28.2
Eu-153	6.1	0.7	0.4	0.8	6.1	1.3	0.4	1.4
Eu-154	13.1	4.1	0.4	4.1	13.4	1.4	0.4	1.4
Eu-155	-4.9	4.9	0.5	4.9	7.2	1.6	0.5	1.7
Gd-155	10.1	1.4	0.4	1.5	15.4	5.0	0.4	5.0
Sr-90	-1.3	15.4	0.2	15.4	-1.3	2.0	0.2	2.0
Mo-95	8.2	13.7	0.3	13.7	18.9	4.5	0.3	4.5
Tc-99	16.9	13.6	0.3	13.6	35.3	4.2	0.3	4.2
Ru-101	27.7	12.9	0.5	12.9	16.3	3.7	0.5	3.8
Ru-106	18.9	5.0	1.1	5.1	-2.0	10.5	1.1	10.6
Rh-103	7.1	12.7	0.2	12.7	23.5	3.9	0.2	3.9
Ag-109	34.7	15.0	0.6	15.0	35.7	4.6	0.6	4.6
Sb-125	75.1	5.4	0.5	5.4	26.1	6.4	0.5	6.4
I-129	18.6	40.4	0.5	40.4	-17.3	6.6	0.5	6.6
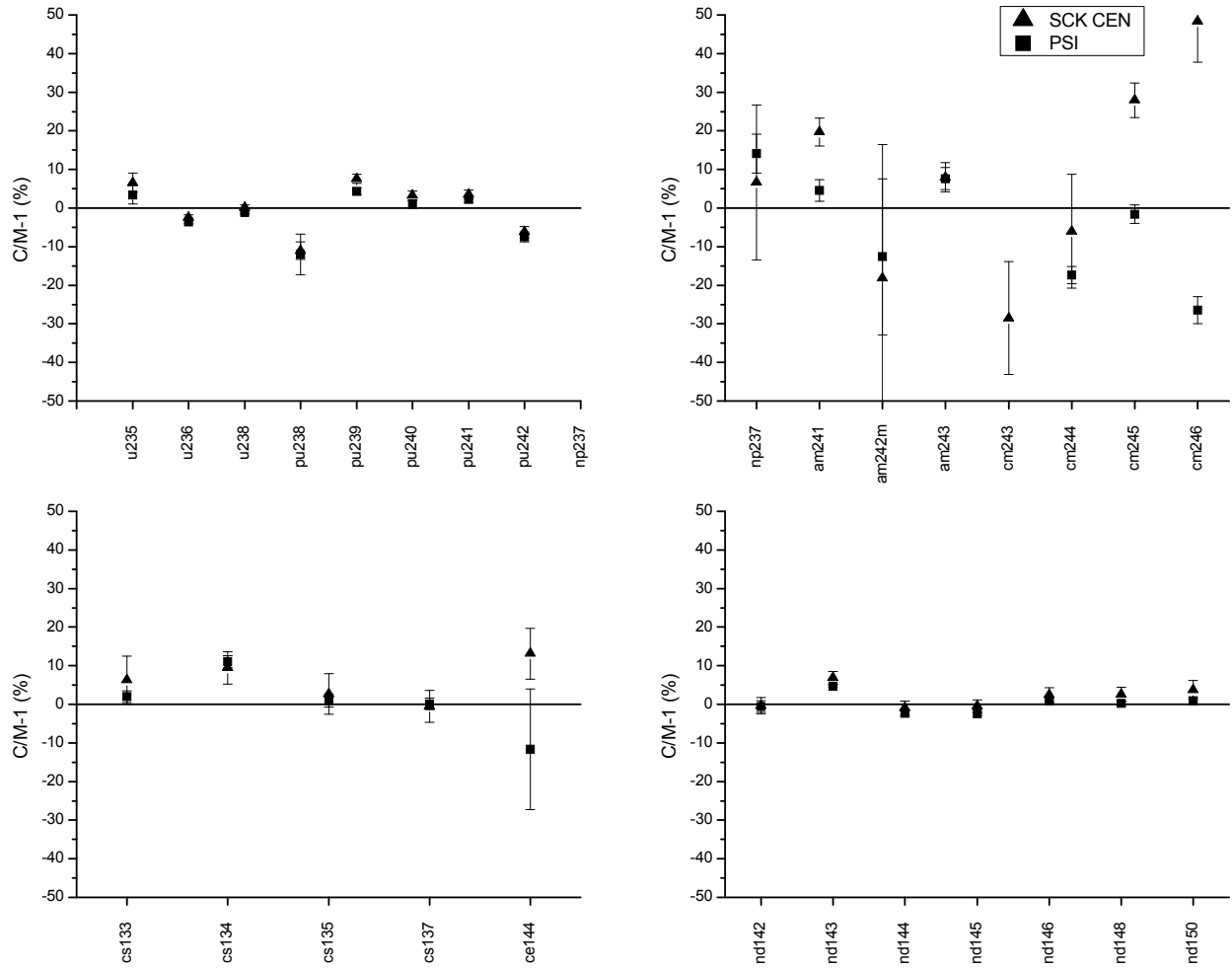
Figure 4-1. Deviation of calculated and measured concentrations for sample KLU1 (U, Pu, Ce, Cs, and Nd).
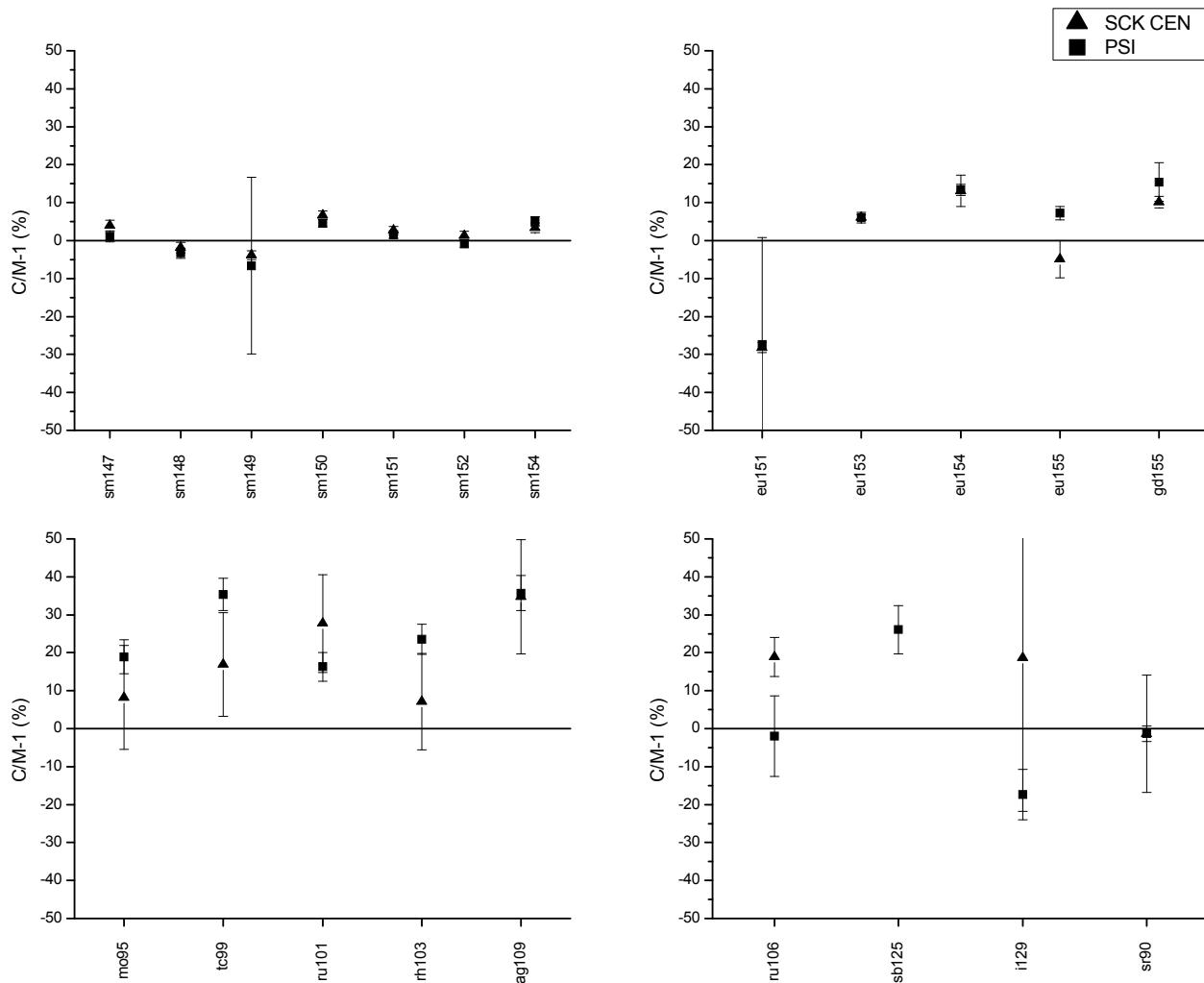
Figure 4-2. Deviation of calculated and measured concentrations for sample KLU1 (Sm, Eu, metallics, and radiological isotopes).

4.2 FORSMARK GE14 SAMPLES

Samples were obtained from fuel rod J8 of Forsmark 3 GE14 assembly GN592. At several nodes, two adjacent samples were analyzed as a monitor of measurement consistency. Note that for these replicate samples (samples 1 and 2, and samples 3 and 7) a single calculation was performed using the measured data for samples 1 and 3.

The tabulated results of deviations between calculations and measurements are presented in Table 4-2. Results for samples 2 and 7 are not listed since they are similar to the replicate samples 1 and 3, obtained from the same elevation of the fuel rod. These results include the relative deviation between the calculated and measured nuclide content, the relative measurement uncertainty, the relative uncertainty associated with the burnup estimate for the sample, and the total combined uncertainty related to the measurements. The burnup values used in the calculations were based on the measured concentrations and uncertainties for ^{148}Nd, a widely used experimental burnup monitor. As observed in Table 4-2, the

uncertainty associated with the burnup estimate is comparable and sometimes larger than the direct measurement uncertainty due to the relatively large uncertainty in the measured ^{148}Nd content.

The following sections discuss the results for selected measured isotopes. The data are presented graphically for the selected nuclides.

4.2.1 Burnup Monitor Isotopes

The burnup values used in the calculations were based on the measured concentration of ^{148}Nd by adjusting the operating power in the simulations such that the calculated ^{148}Nd content matched the measured value for each sample. In the case of the measurements performed by Studsvik, the ^{148}Nd uncertainties (95% confidence) were large, varying from about 4% for some samples to more than 14% for other samples (see Table 4-2). To provide cross checks of sample burnup, other fission product burnup monitors with generally lower measurement uncertainty were evaluated to verify the consistency of the burnup estimated using ^{148}Nd burnup. Other isotopes included ^{137}Cs, ^{139}La, and ^{146}Nd—all long-lived or stable fission products with concentrations that are relatively proportional to burnup.

The burnup uncertainties applied in this study are based exclusively on ^{148}Nd, although the application of other burnup indicators may reduce the error in the burnup estimate. Therefore, the uncertainties given in this report are expected to be conservative. The sample burnup predicted based on ^{148}Nd is listed in Table 4-2. The values are within 1% of the ^{148}Nd burnup values determined by Studsvik.

The deviations for the fission products ^{148}Nd, ^{137}Cs, ^{139}La, and ^{146}Nd are shown in Figure 4-3. The calculations were normalized to the ^{148}Nd content; therefore, there are no deviations for ^{148}Nd. Both ^{137}Cs and ^{139}La are also widely used as burnup indicators. Fission product ^{146}Nd is also used as a burnup indicator, as it is long lived and is measured with relatively high accuracy due to its higher isotopic concentration in the samples relative to ^{148}Nd. Notwithstanding the relatively large measurement errors, the use of ^{148}Nd for burnup produces generally good agreement for the other burnup indicators, particularly ^{137}Cs and ^{146}Nd. The calculated results for ^{139}La are systematically low, suggesting the burnup in the samples is underestimated. However, the measurement errors for ^{139}La (~12%) are significantly larger than for ^{137}Cs (~2%) and all ^{139}La results are in agreement within the experimental uncertainties. Based on these observations, the burnup based on ^{148}Nd was considered to be reliable for application in this study.

Data evaluations to provide improved burnup estimates with reduced uncertainties for the samples based on multiple burnup indicators are continuing under the experimental program.

4.2.2 Uranium Isotopes

The deviations for the major uranium isotopes are shown in Figure 4-4 as a function of axial elevation of each sample. The results are generally within the estimated uncertainties. The results for ^{235}U exhibit large variability; however, there is a large uncertainty associated with the burnup estimate of the samples (see Table 4-2). At the high burnup levels of these samples, a 1% change in the burnup can cause a 6% change in the ^{235}U concentration. The uncertainty in the ^{235}U results that is attributed to the burnup uncertainties (from ^{148}Nd) was greater than 20% for most samples. This result highlights the importance of extremely accurate measurements of the burnup indicators of the fuel to validate nuclides such as ^{235}U.

4.2.3 Plutonium Isotopes

The deviations for the plutonium isotopes are shown in Figure 4-5 (^{238}Pu is included in Figure 4-6). The results show consistent behavior for all samples. All isotopes are generally predicted within about 10% of measurements. The ^{239}Pu and ^{241}Pu content is generally predicted within experimental uncertainty, with a small under prediction of less than 5%. The results for ^{240}Pu are over predicted but are generally within about 10% of measurement. The results for ^{238}Pu are under predicted by about 10% for most samples; however, the uncertainty due to the burnup error is significant and most results are within experimental uncertainty.

The ^{239}Pu result for sample 4 (~2500 mm) exhibits the largest deviation of all samples, showing an under prediction of about 10%. Further review of this sample indicates it was obtained at an elevation approximately 250 mm above the transition height of the dominant and vanished axial zones. The GE14 assembly has a plenum region containing additional hardware above the partial-length fuel rods, with a length of about 300 mm, placing sample 4 very near the plenum region. The under prediction of ^{239}Pu suggests that the actual spectrum in node 17 was harder (i.e., less moderation) than was present in the model. This result is consistent with the presence of plenum hardware, not included in the model. Additional information of the plenum region may be used to improve the model representation and neutronic environment of this region.

4.2.4 Minor Actinides

Results for the minor actinides ^{237}Np, ^{238}Pu, ^{241}Am and ^{243}Am are shown in Figure 4-6. The results for ^{237}Np are within 5% of measurement on average, and ^{243}Am results are within the experimental uncertainties. The ^{241}Am results show good agreement with measurements; generally within 10% for all samples. The uncertainties for these nuclides are large, with significant contributions from both the measurement error and burnup estimates (see Table 4-2).

4.2.5 Cesium Isotopes

The cesium results shown in Figure 4-7 are generally well predicted with the exception of ^{134}Cs, consistently under predicted by more than 10% on average. Both ^{134}Cs and ^{137}Cs are important radiological fission products and gamma emitters, and contribute to decay heat. The ^{133}Cs isotope has a large neutron capture cross section and is an important fission product in nuclear criticality safety involving irradiated fuel. Cesium-133 is well predicted and is within 7% of measurements on average. The ^{135}Cs isotope, a long-lived fission product important to waste management applications, is predicted to within 1% of measurements.

4.2.6 Neodymium Isotopes

Neodymium results are shown in Figure 4-8. The results for ^{148}Nd are not shown since they show no deviation because the calculations were normalized to measured ^{148}Nd. Both ^{143}Nd and ^{145}Nd are important in nuclear criticality safety, and they exhibit a small over prediction on average of about 8% and 3%, respectively.

4.2.7 Samarium Isotopes

The samarium isotopes, shown in Figure 4-9 (^{152}Sm is included in Figure 4-10), are important to nuclear criticality safety. The results are generally predicted within experimental uncertainty. Samarium-149, and

important fission product in burnup credit, is under predicted by 12% on average. The reported relative uncertainty in measured ^{149}Sm was large, up to 16% due to its relatively low isotopic concentration in the samples, and may have contributed to the observed deviations.

4.2.8 **Europium and Gadolinium Isotopes**

Europium and gadolinium results are shown in Figure 4-10. The results are generally within the experimental uncertainties. The results for ^{155}Eu and ^{155}Gd are over predicted by about 10% on average. The consistent behavior of these nuclides is expected since ^{155}Gd is the decay daughter of ^{155}Eu. The agreement indicates the measurements are self-consistent.

4.2.9 **Metallic Isotopes and Other Fission Products**

Results for the metallic fission products ^{95}Mo, ^{99}Tc, ^{103}Rh, and ^{109}Ag are presented in Figure 4-11. Results for ^{95}Mo and ^{99}Tc are over predicted by about 10%, and most results are within experimental uncertainty. The result for ^{103}Rh, an important fission product in nuclear criticality safety, is in good agreement with experiment, within 2% on average. The results for ^{109}Ag are over predicted by upwards of 30%; however, the results show significant variability and large error bars. The over prediction may be related to problems associated with the stability of ^{109}Ag during the measurements and incomplete recovery (i.e., low measured concentrations).

Results for radiological isotopes ^{90}Sr, ^{106}Ru, ^{125}Sb, and ^{129}I are shown in Figure 4-12. All nuclides are generally within the experimental errors but show considerable variability and have large measurement uncertainties.

Table 4-2. Results for Forsmark 3 GE14 Samples

Sample ID	GN592-J8-1				GN592-J8-3				GN592-J8-4			
Burnup (GWd/MTU)	50.86				51.90				56.65			
Elevation (mm)	1842–1852				712–722				2503–2513			
		2σ uncertainties				2σ uncertainties				2σ uncertainties		
Nuclide	C/M-1 (%)	Meas. (%)	Burnup (%)	Total (%)	C/M-1 (%)	Meas. (%)	Burnup (%)	Total (%)	C/M-1 (%)	Meas. (%)	Burnup (%)	Total (%)
U-234	0.2	7.8	3.5	8.5	-7.5	7.4	5.0	9.0	-5.0	8.0	14.7	16.8
U-235	-3.1	3.2	13.4	13.8	-22.2	3.2	21.0	21.3	-27.1	3.3	62.0	62.1
U-236	-6.4	3.2	1.3	3.4	-4.3	3.1	1.0	3.3	-3.0	3.2	3.8	4.9
U-238	-0.6	2.0	0.0	2.0	-1.0	2.0	0.6	2.1	-0.9	2.0	1.2	2.3
Pu-238	-13.1	5.6	9.4	10.9	-7.5	23.8	12.7	27.0	-6.8	3.8	29.0	29.2
Pu-239	-3.9	3.8	4.5	5.9	-3.1	2.9	2.0	3.6	-9.9	3.1	15.1	15.4
Pu-240	9.2	3.8	2.4	4.5	7.6	3.3	2.5	4.2	12.2	3.2	4.9	5.9
Pu-241	-4.6	4.0	0.0	4.0	-1.1	3.3	1.0	3.4	-5.4	3.6	3.1	4.8
Pu-242	-2.8	3.9	10.2	10.9	8.9	3.2	12.1	12.5	13.7	3.6	33.6	33.7
Np-237	2.4	12.4	3.5	12.9	9.4	12.5	5.8	13.8	7.8	12.3	11.2	16.6
Am-241	6.3	3.5	7.6	8.3	8.1	6.1	14.3	15.6	3.2	5.5	14.5	15.5
Am-243	7.2	10.4	12.3	16.1	26.9	6.6	16.3	17.6	22.3	8.9	41.3	42.2
Cm-244	41.7	13.6	16.7	21.6	94.4	13.5	23.7	27.3	88.5	12.6	58.3	59.7
Cm-246	43.2	20.7	27.7	34.6	75.6	44.4	36.1	57.2	84.6	32.6	105.5	110.4
Cs-133	-12.1	2.4	3.6	4.3	-1.6	2.8	4.0	4.9	2.7	2.8	11.5	11.9
Cs-134	-16.6	4.3	2.3	4.8	-4.9	4.9	0.7	4.9	-6.2	4.0	10.0	10.8
Cs-135	-0.2	2.6	6.1	6.6	-1.1	2.7	7.6	8.1	-1.5	3.0	20.1	20.4
Cs-137	-5.8	2.1	3.9	4.4	0.2	2.6	4.3	5.0	3.3	2.5	14.1	14.3
Ce-140	-5.1	3.2	4.6	5.6	-0.5	7.3	5.3	9.0	3.7	10.8	15.7	19.1
Ce-142	-8.9	3.2	4.4	5.4	-1.8	6.7	5.1	8.4	0.1	10.8	14.4	18.0
Ce-144	-35.2	19.9	9.8	22.2	-38.6	19.2	21.8	29.0	-36.5	17.0	31.5	35.8
La-139	-7.0	12.3	4.2	13.0	-6.0	12.9	4.7	13.7	-4.3	12.2	14.4	18.9
Nd-142	-3.5	8.9	11.1	14.2	7.7	4.2	14.1	14.7	12.6	3.9	41.8	41.9
Nd-143	11.3	4.7	0.7	4.8	6.6	4.4	1.2	4.6	7.8	4.9	3.3	5.9
Nd-144	0.6	3.3	7.6	8.3	5.9	4.7	9.5	10.6	10.8	5.0	26.2	26.7
Nd-145	3.5	3.6	3.5	5.0	4.5	6.0	3.4	6.9	8.4	7.7	10.5	13.0
Nd-146	2.3	2.9	5.3	6.1	9.0	3.0	6.3	7.0	12.6	4.1	19.0	19.4
Nd-148	0.0	4.6	4.6	6.5	0.0	4.8	4.8	6.8	0.0	15.5	15.5	22.0
Nd-150	-1.7	7.1	5.0	8.7	5.2	3.0	6.0	6.7	1.8	7.2	17.5	19.0
Sm-147	9.9	4.5	8.2	9.3	12.2	7.6	11.4	13.7	22.0	11.4	25.3	27.8
Sm-148	-5.8	4.7	7.9	9.2	7.3	7.1	10.4	12.6	10.8	11.2	27.9	30.1
Sm-149	-11.7	8.7	6.1	10.6	-12.8	11.1	5.8	12.5	-23.4	16.0	19.1	24.9
Sm-150	2.8	4.8	3.7	6.1	11.9	7.3	3.9	8.3	16.6	10.8	11.4	15.7
Sm-151	-8.8	6.7	2.3	7.1	0.6	22.2	0.0	22.2	-5.6	18.2	7.2	19.6
Sm-152	5.9	4.1	3.6	5.4	2.9	6.3	3.1	7.0	15.3	6.7	12.0	13.8
Sm-154	0.0	10.2	6.3	12.0	5.0	10.7	6.7	12.6	12.1	13.1	20.7	24.5
Eu-153	11.2	3.7	4.8	6.1	16.8	7.7	5.6	9.5	19.1	2.4	15.4	15.6
Eu-154	10.6	9.1	3.1	9.6	22.4	11.1	5.3	12.3	12.0	8.7	9.7	13.0
Eu-155	18.5	33.3	5.8	33.8	19.9	10.3	5.3	11.6	9.7	11.0	18.0	21.0
Gd-154	15.9	14.3	15.5	21.1	22.1	16.7	24.1	29.3	15.6	13.3	50.9	52.7
Gd-155	10.3	14.8	3.1	15.1	11.7	11.5	10.9	15.9	11.2	6.7	7.6	10.1
Gd-156	-6.6	11.6	11.9	16.6	6.6	8.7	15.6	17.9	6.2	3.6	43.0	43.2
Gd-158	0.0	19.4	8.7	21.2	14.6	7.4	11.4	13.6	11.7	17.1	33.7	37.8
Mo-94	-99.7	44.1	10.6	45.4	-99.5	27.0	14.2	30.5	-99.6	26.3	38.1	46.3
Mo-95	8.8	9.2	4.2	10.1	8.6	7.2	5.0	8.7	27.5	15.6	13.0	20.3
Mo-96	-19.2	28.2	10.1	29.9	-20.0	26.8	13.5	30.0	9.8	6.7	37.1	37.7
Mo-97	5.9	7.7	4.2	8.7	5.8	6.9	4.9	8.5	20.6	5.7	15.3	16.3
Mo-98	-2.5	8.9	4.4	9.9	-0.5	6.9	5.2	8.7	10.5	7.4	15.5	17.2
Mo-100	-7.7	9.4	4.7	10.5	-5.6	7.4	5.4	9.2	3.9	8.0	16.4	18.2
Sr-90	-10.7	11.5	2.4	11.8	-7.2	11.7	2.1	11.9	-8.1	11.9	7.9	14.3
Tc-99	3.8	11.7	3.7	12.3	4.5	11.6	4.2	12.3	9.6	11.8	11.8	16.7

42

Table 4-2. (continued)

Sample ID	GN592-J8-1				GN592-J8-3				GN592-J8-4			
Burnup (GWd/MTU)	50.86				51.90				56.65			
Elevation (mm)	1842–1852				712–722				2503–2513			
		2σ uncertainties				2σ uncertainties				2σ uncertainties		
Nuclide	C/M-1 (%)	Meas. (%)	Burnup (%)	Total (%)	C/M-1 (%)	Meas. (%)	Burnup (%)	Total (%)	C/M-1 (%)	Meas. (%)	Burnup (%)	Total (%)
Ru-101	-6.1	11.9	4.7	12.8	-6.5	11.8	5.1	12.9	2.4	11.8	15.8	19.7
Ru-102	2.3	11.5	5.0	12.6	2.2	11.6	6.2	13.2	15.4	13.1	18.5	22.6
Ru-104	-31.2	11.6	5.8	13.0	-30.2	11.6	7.6	13.9	-20.5	11.8	20.3	23.5
Ru-106	4.3	16.5	3.5	16.9	3.7	15.9	10.3	18.9	23.5	16.9	8.8	19.0
Rh-103	2.2	11.9	2.9	12.2	-0.6	11.8	3.6	12.3	4.3	15.8	7.9	17.7
Pd-105	8.4	11.6	5.9	13.0	10.5	12.2	8.2	14.7	19.6	12.0	21.3	24.4
Pd-107	0.6	13.5	7.2	15.3	5.4	14.6	9.1	17.2	11.9	12.6	25.3	28.3
Pd-108	0.6	11.8	7.6	14.0	2.5	11.6	9.5	15.0	15.8	12.5	26.6	29.4
Pd-110	-46.1	14.2	7.7	16.2	-44.3	11.6	9.7	15.1	-39.4	13.3	26.8	29.9
Ag-109	28.6	12.6	6.2	14.0	29.6	11.8	7.3	13.9	32.8	12.2	21.0	24.3
Cd-111	28.8	13.5	7.8	15.6	34.7	13.6	10.1	16.9	49.6	15.6	27.4	31.6
Cd-112	-48.9	13.5	7.3	15.3	-49.2	17.0	9.3	19.4	-42.6	13.5	26.0	29.3
Cd-114	52.1	12.7	6.5	14.3	48.1	15.2	8.1	17.2	65.4	14.4	23.7	27.7
Sb-125	-15.5	33.3	0.7	33.3	-18.6	33.3	3.4	33.5	-18.5	42.9	1.9	42.9
I-129	-23.4	42.2	5.0	42.5	-19.5	36.1	5.9	36.6	16.2	35.7	17.5	39.8

Sample ID	GN592-J8-5				GN592-J8-6				GN592-J8-8			
Burnup (GWd/MTU)	43.53				43.12				38.20			
Elevation (mm)	3277–3287				397–407				3384–3394			
U-234	0.2	8.0	7.0	10.6	-1.9	7.8	6.4	10.1	4.0	8.7	3.3	9.3
U-235	-2.4	3.1	24.9	25.1	-4.4	3.1	26.4	26.6	5.2	3.1	10.9	11.3
U-236	-3.5	3.2	4.0	5.1	-3.5	3.1	3.3	4.6	-1.5	3.3	2.9	4.4
U-238	-0.3	2.0	0.0	2.0	-0.5	2.0	0.0	2.0	-0.3	2.0	0.3	2.0
Pu-238	-16.1	3.7	23.4	23.7	-10.6	4.1	25.0	25.4	-20.0	11.7	13.6	17.9
Pu-239	-2.2	3.1	6.6	7.3	-2.6	3.0	1.6	3.4	0.8	2.9	2.4	3.8
Pu-240	9.1	3.2	7.4	8.1	1.4	3.1	6.2	7.0	7.1	3.0	4.9	5.7
Pu-241	-4.2	3.4	4.6	5.7	-4.7	3.4	4.4	5.6	-2.9	3.2	3.3	4.6
Pu-242	-3.2	3.4	25.3	25.5	-4.8	4.0	20.4	20.7	-5.3	3.7	14.1	14.5
Np-237	2.0	12.7	11.1	16.9	2.4	12.6	9.7	15.9	0.0	12.6	5.9	13.9
Am-241	10.6	4.1	9.5	10.3	5.9	3.3	27.8	28.0	5.5	7.4	11.1	13.3
Am-243	10.0	4.7	32.0	32.3	-4.6	23.1	30.5	38.2	-21.2	47.1	18.2	50.5
Cm-244	39.3	13.1	43.4	45.4	48.1	13.6	42.1	44.2	24.7	12.1	24.8	27.6
Cm-246	9.5	32.0	67.9	75.1	18.3	87.5	64.6	108.7	-17.8	30.8	38.3	49.1
Cs-133	-5.3	2.9	9.2	9.6	-8.1	2.9	6.7	7.3	-6.1	2.8	5.0	5.7
Cs-134	-17.3	5.6	14.3	15.4	-12.9	6.5	2.4	6.9	-16.6	13.8	6.2	15.1
Cs-135	-1.4	3.0	11.1	11.5	-2.8	2.8	13.1	13.4	-0.5	2.8	6.4	7.0
Cs-137	-5.9	2.9	9.7	10.2	-7.9	2.4	7.0	7.4	-6.8	2.5	5.2	5.8
Ce-140	-7.1	3.8	10.8	11.4	-12.9	6.5	8.3	10.6	-11.6	8.2	5.6	10.0
Ce-142	-3.9	3.1	10.2	10.7	-7.2	3.4	7.9	8.6	-8.2	5.9	5.5	8.0
Ce-144	-4.0	17.8	4.2	18.3	-10.8	16.9	35.5	39.3	-1.3	16.2	6.9	17.6
La-139	-11.8	12.5	10.1	16.1	-13.5	12.4	7.9	14.7	-15.5	12.5	5.5	13.7
Nd-142	-17.4	10.8	26.0	28.2	-14.8	5.0	22.7	23.3	-34.9	5.7	13.8	15.0
Nd-143	9.0	4.2	3.4	5.4	7.1	4.3	1.0	4.4	7.4	4.2	2.3	4.8
Nd-144	1.4	4.5	15.9	16.5	-2.8	3.3	15.4	15.8	-2.1	4.0	9.4	10.2
Nd-145	2.1	5.7	8.1	9.9	-2.4	5.2	6.2	8.1	2.9	3.9	5.0	6.3
Nd-146	1.5	3.3	12.2	12.6	0.6	3.0	10.6	11.0	1.9	3.0	6.7	7.3
Nd-148	0.1	11.1	11.1	15.7	-0.1	7.4	7.4	10.5	0.0	5.6	5.6	7.9
Nd-150	-4.2	6.6	11.8	13.5	-6.0	5.0	9.9	11.1	-1.5	14.6	6.4	16.0

Table 4-2. (continued)

Sample ID	GN592-J8-5				GN592-J8-6				GN592-J8-8			
Burnup (GWd/MTU)	43.53				43.12				38.20			
Elevation (mm)	3277–3287				397–407				3384–3394			
		2σ uncertainties				2σ uncertainties				2σ uncertainties		
	C/M-1	Meas.	Burnup	Total	C/M-1	Meas.	Burnup	Total	C/M-1	Meas.	Burnup	Total
Nuclide	(%)	(%)	(%)	(%)	(%)	(%)	(%)	(%)	(%)	(%)	(%)	(%)
Sm-147	-14.1	5.5	14.2	15.2	-14.0	10.1	20.1	22.5	-15.1	8.3	10.1	13.1
Sm-148	-0.2	6.4	18.4	19.5	1.0	10.2	17.7	20.4	-5.2	6.3	10.3	12.1
Sm-149	-12.5	16.0	8.4	18.1	-10.4	35.3	11.3	37.1				
Sm-150	6.4	7.0	9.7	12.0	7.8	10.4	7.1	12.6	7.4	6.7	5.3	8.6
Sm-151	15.5	22.2	3.1	22.4	20.2	28.6	0.0	28.6	1.5	20.0	1.2	20.0
Sm-152	8.0	6.0	7.9	9.9	0.7	9.7	5.0	10.9	6.5	3.2	4.3	5.4
Sm-154	-5.4	8.0	13.7	15.9	-7.6	12.5	12.0	17.3	-9.9	9.1	7.6	11.8
Eu-153	-0.2	17.2	12.6	21.3	8.9	5.9	10.4	12.0	8.4	6.7	7.5	10.0
Eu-154	8.8	22.2	12.5	25.5	14.5	6.7	11.0	12.9	1.0	12.5	7.7	14.7
Eu-155	-4.6	33.3	16.1	37.0	13.3	17.0	10.2	19.9	-2.5	12.5	9.2	15.5
Gd-154	14.4	18.2	28.5	33.8	23.8	11.1	41.7	43.1	9.5	22.2	19.7	29.7
Gd-155	19.8	10.0	3.3	10.5	9.2	14.6	29.2	32.6	3.4	10.5	3.5	11.1
Gd-156	-6.7	6.3	27.7	28.4	-4.4	9.8	25.6	27.4	-13.4	6.2	14.6	15.8
Gd-158	9.9	20.0	20.4	28.6	9.8	11.1	17.7	20.9	0.3	11.8	10.4	15.7
Mo-94	-99.8	19.5	24.9	31.7	-99.9	48.5	23.7	54.0	-99.9	17.4	13.8	22.2
Mo-95	2.1	13.0	8.6	15.6	19.3	42.8	8.3	43.6	4.9	5.7	5.3	7.8
Mo-96	-64.9	27.6	23.6	36.3	-28.2	66.7	21.4	70.0	-29.6	6.3	12.6	14.1
Mo-97	-0.9	4.9	10.2	11.3	14.6	42.7	7.6	43.4	-1.0	5.5	5.4	7.7
Mo-98	-1.1	15.2	10.5	18.4	6.8	42.7	9.2	43.7	-7.5	6.0	6.0	8.5
Mo-100	-7.7	15.0	11.0	18.6	0.5	42.8	8.8	43.7	-13.8	5.7	5.8	8.1
Sr-90	-12.9	12.4	7.1	14.3	-12.0	11.6	3.8	12.2	-7.4	13.8	3.8	14.3
Tc-99	0.8	11.6	9.8	15.2	-2.3	12.2	6.8	14.0	-2.0	11.6	5.1	12.7
Ru-101	-8.9	11.8	10.6	15.8	-12.2	12.2	8.8	15.1	-13.2	11.8	6.0	13.2
Ru-102	-15.3	41.5	12.4	43.3	-11.2	12.3	9.7	15.7	-13.1	11.6	6.3	13.2
Ru-104	-32.5	11.7	14.1	18.4	-36.7	12.3	11.8	17.1	-35.7	11.8	7.3	13.9
Ru-106	10.1	16.8	5.9	17.8	6.6	17.8	16.8	24.5	1.6	17.5	0.3	17.5
Rh-103	-1.7	12.0	7.5	14.1	-7.7	12.2	6.5	13.8	-4.3	11.6	4.6	12.5
Pd-105	4.5	11.7	14.6	18.7	-0.5	12.5	13.3	18.2	2.2	12.1	8.3	14.7
Pd-107	-0.9	12.8	16.8	21.1	-9.2	12.1	14.8	19.1	-10.1	12.0	9.1	15.1
Pd-108	-7.3	12.7	17.7	21.8	-11.9	12.5	15.8	20.1	-10.1	12.1	9.5	15.4
Pd-110	-49.3	12.1	18.1	21.8	-50.9	12.8	15.8	20.4	-50.5	12.4	9.6	15.7
Ag-109	18.5	15.4	14.9	21.4	1.7	12.6	12.8	17.9	2.8	14.0	8.2	16.2
Cd-111	22.0	20.7	17.9	27.4	11.0	16.0	16.0	22.6	22.0	24.9	9.6	26.7
Cd-112	-56.2	11.8	16.9	20.6	-58.4	17.5	14.5	22.7	-60.9	11.8	8.8	14.7
Cd-114	21.8	12.9	15.1	19.9	28.2	19.3	13.0	23.3	27.8	26.0	8.0	27.2
Sb-125	37.4	15.9	4.4	16.5	24.7	16.1	5.8	17.1	23.5	15.9	1.5	16.0
I-129	-17.0	42.0	11.8	43.6	-41.9	57.3	9.9	58.1	-34.5	42.1	6.6	42.6
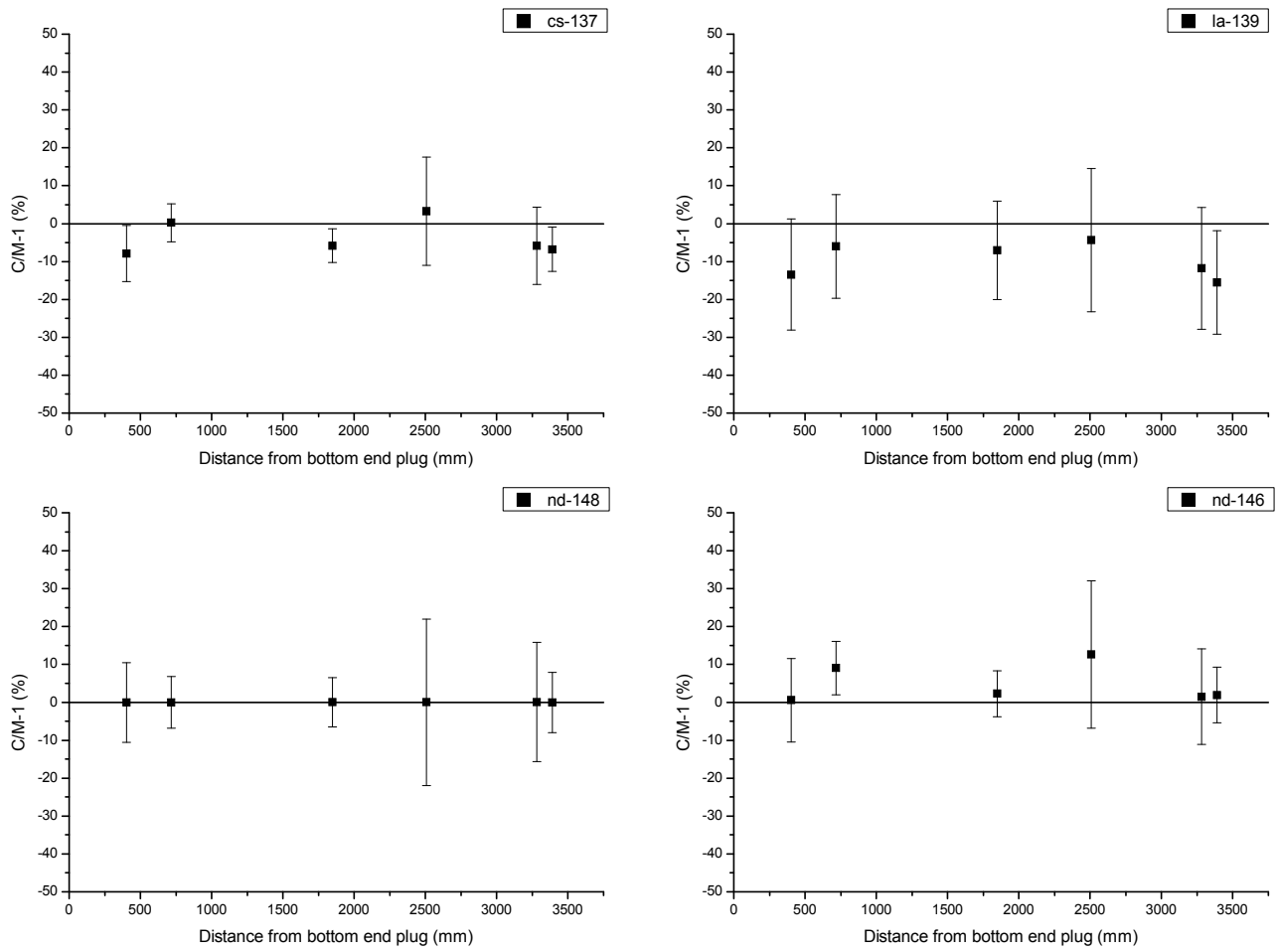
Figure 4-3. Deviations of calculated and measured concentrations for GE14 samples (^{137}Cs, ^{139}La, ^{146}Nd, and ^{148}Nd).
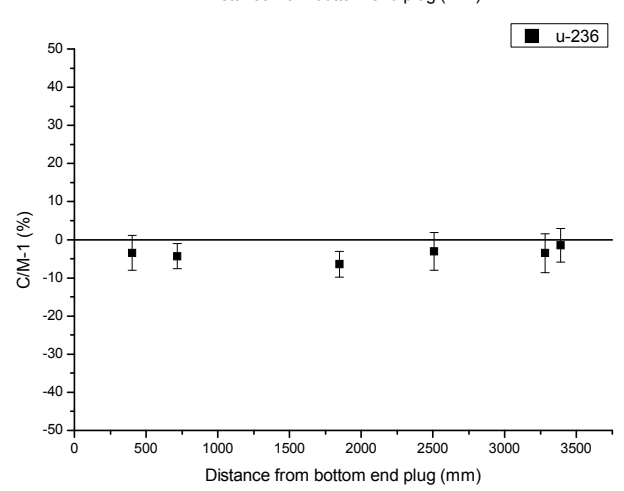
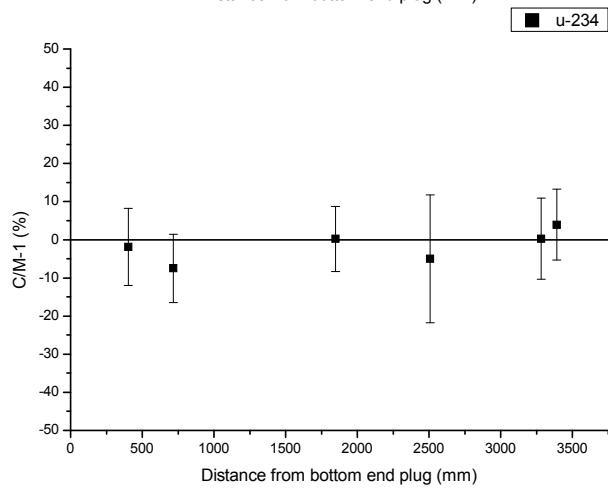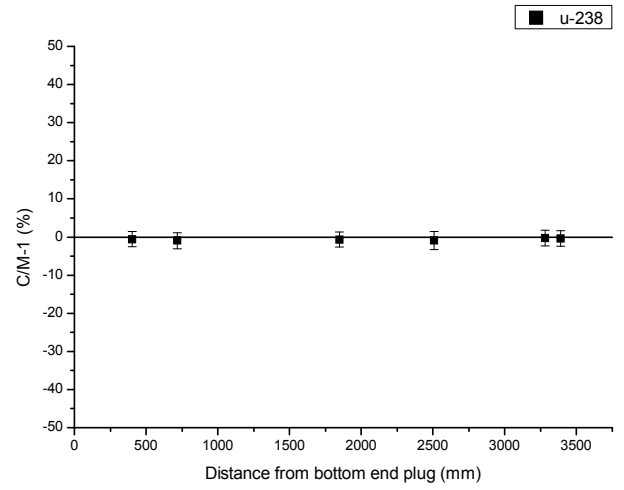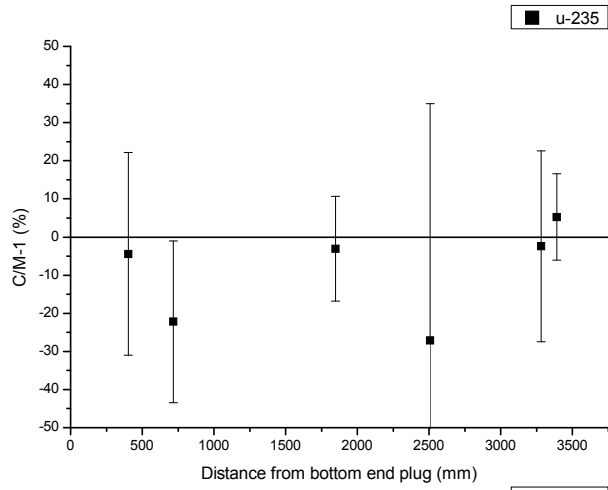**Figure 4-4. Deviations of calculated and measured concentrations for GE14 samples (^{234}U, ^{235}U, ^{236}U, and ^{238}U).**
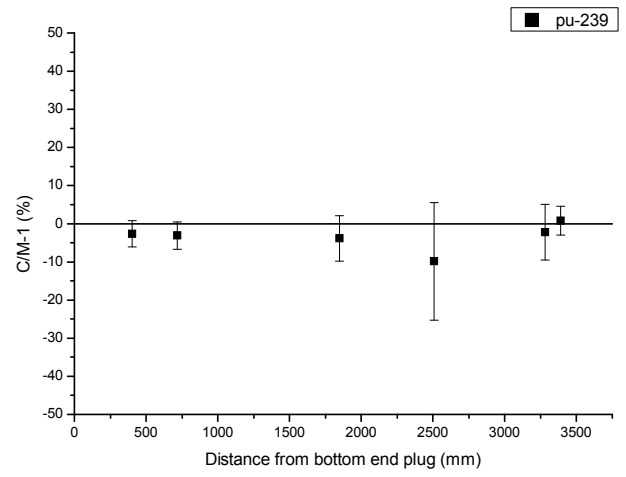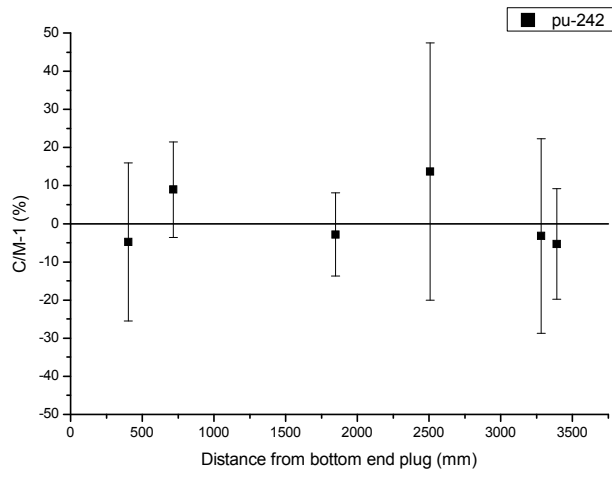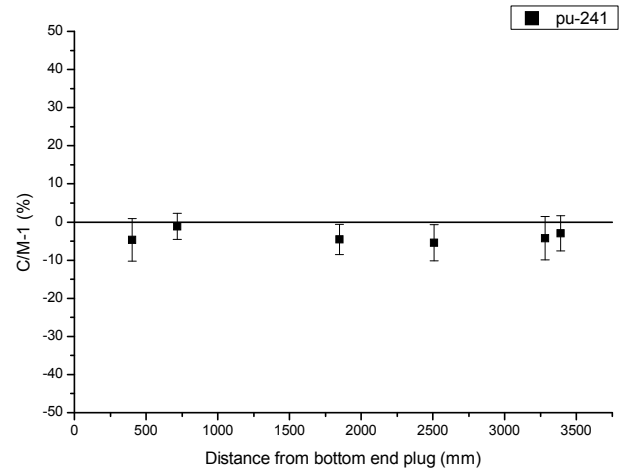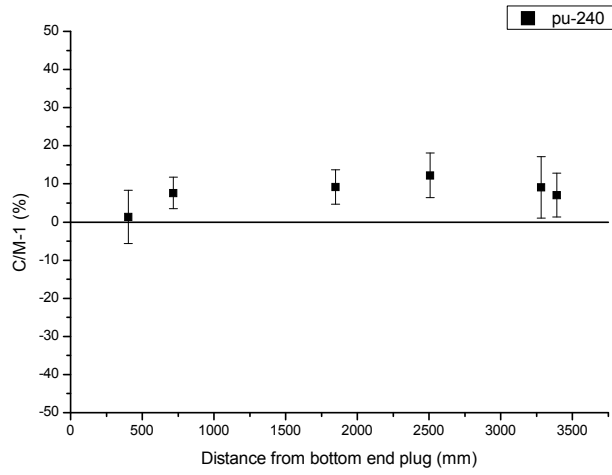
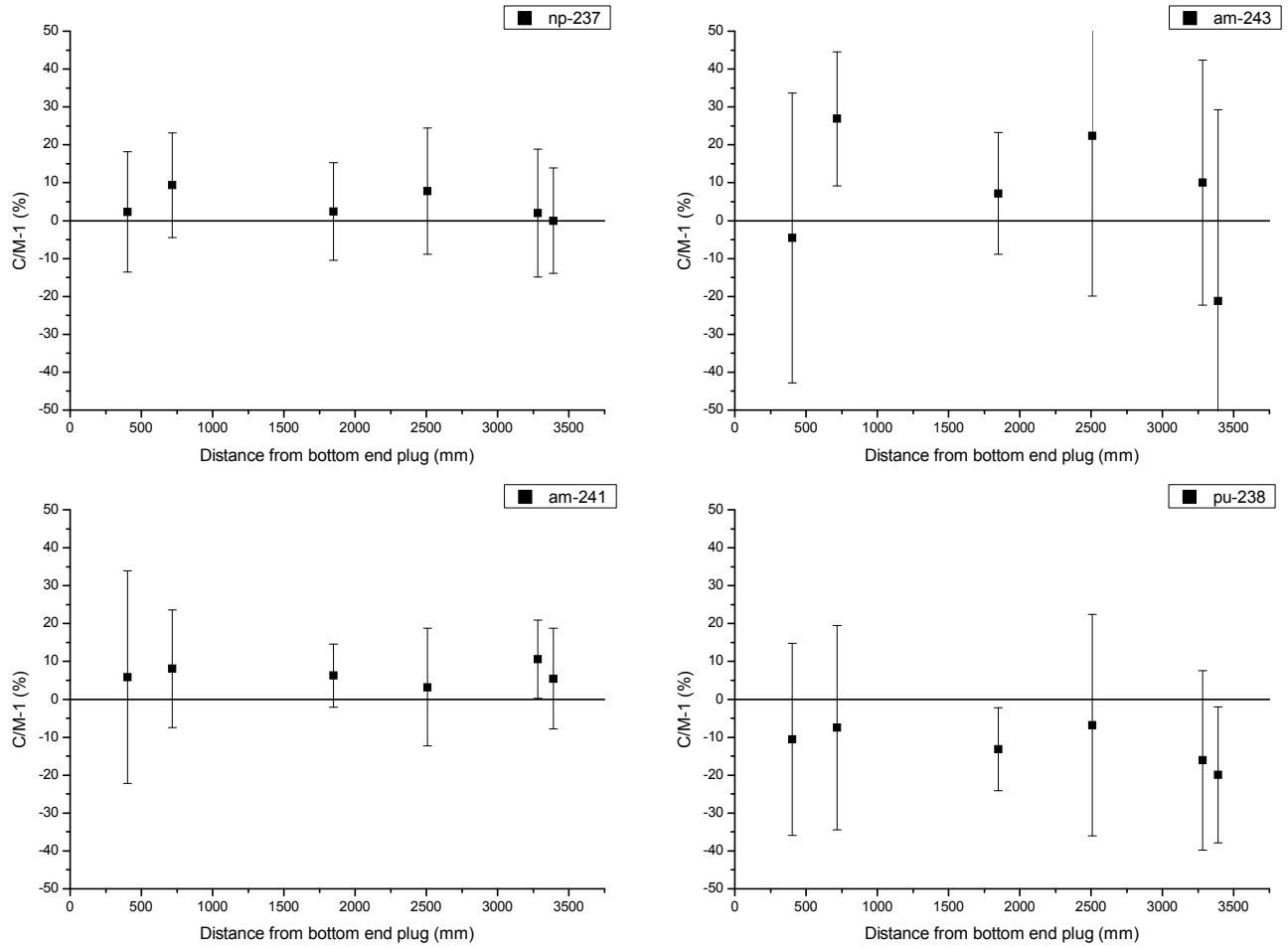**Figure 4-5. Deviations of calculated and measured concentrations for GE14 samples (^{239}Pu, ^{240}Pu, ^{241}Pu, and ^{242}Pu).**

Figure 4-6. **Deviations of calculated and measured concentrations for GE14 samples (^{237}Np, ^{241}Am, ^{243}Am, and ^{238}Pu).**

Figure 4-7. Deviations of calculated and measured concentrations for GE14 samples (^{133}Cs, ^{134}Cs, ^{135}Cs, and ^{137}Cs).

Figure 4-8. Deviations of calculated and measured concentrations for GE14 samples (^{143}Nd, ^{144}Nd, ^{145}Nd, and ^{146}Nd).
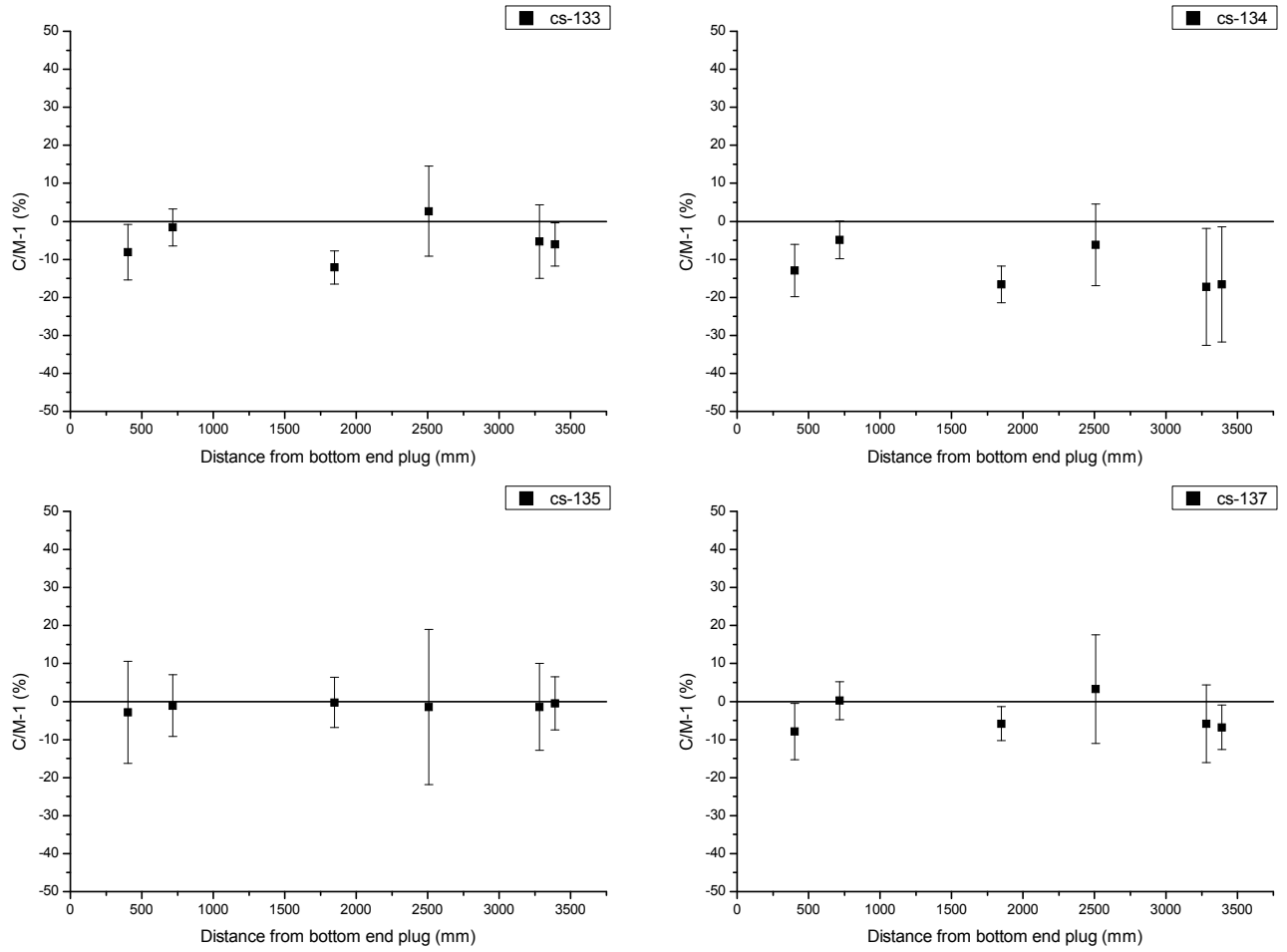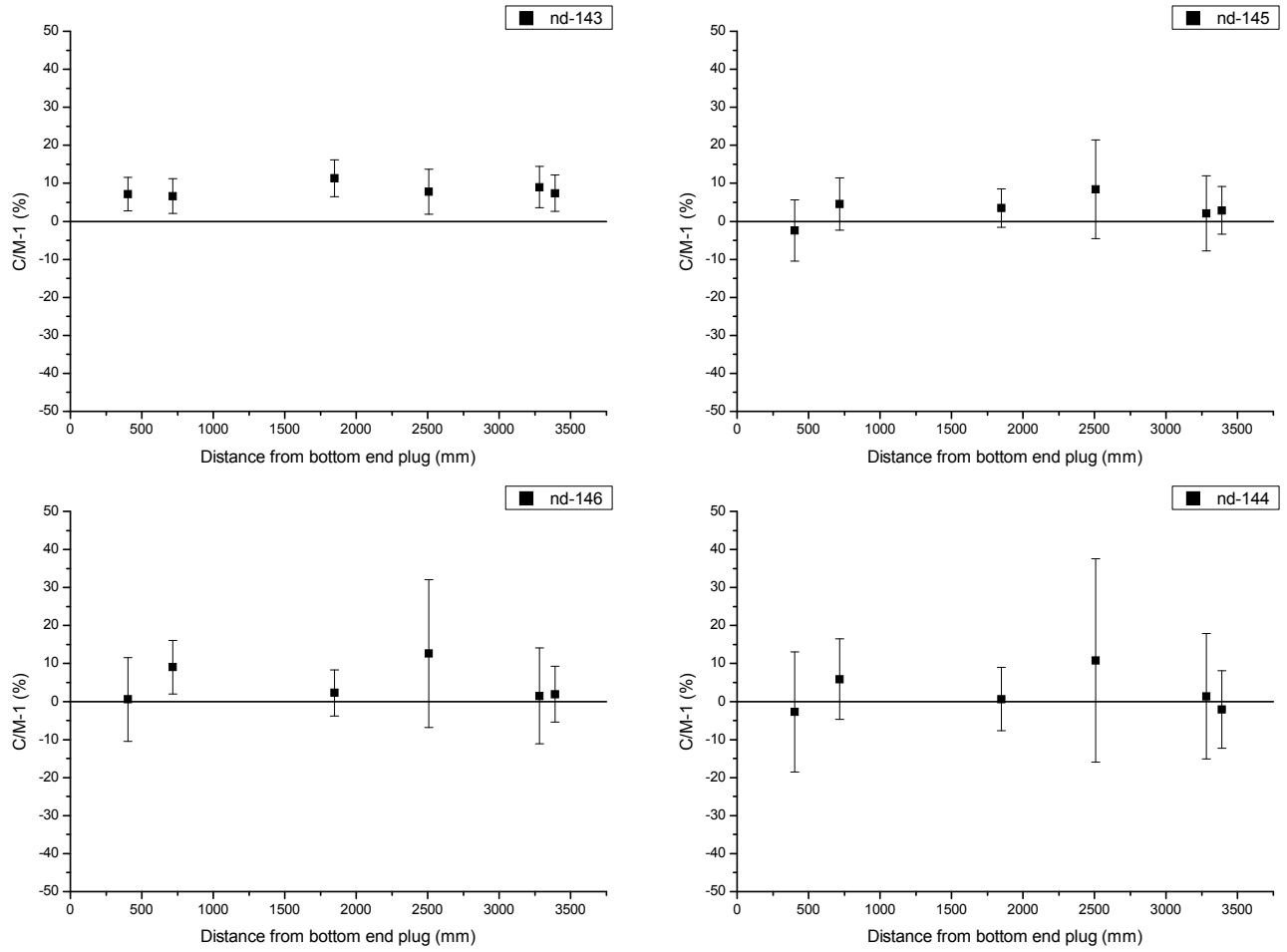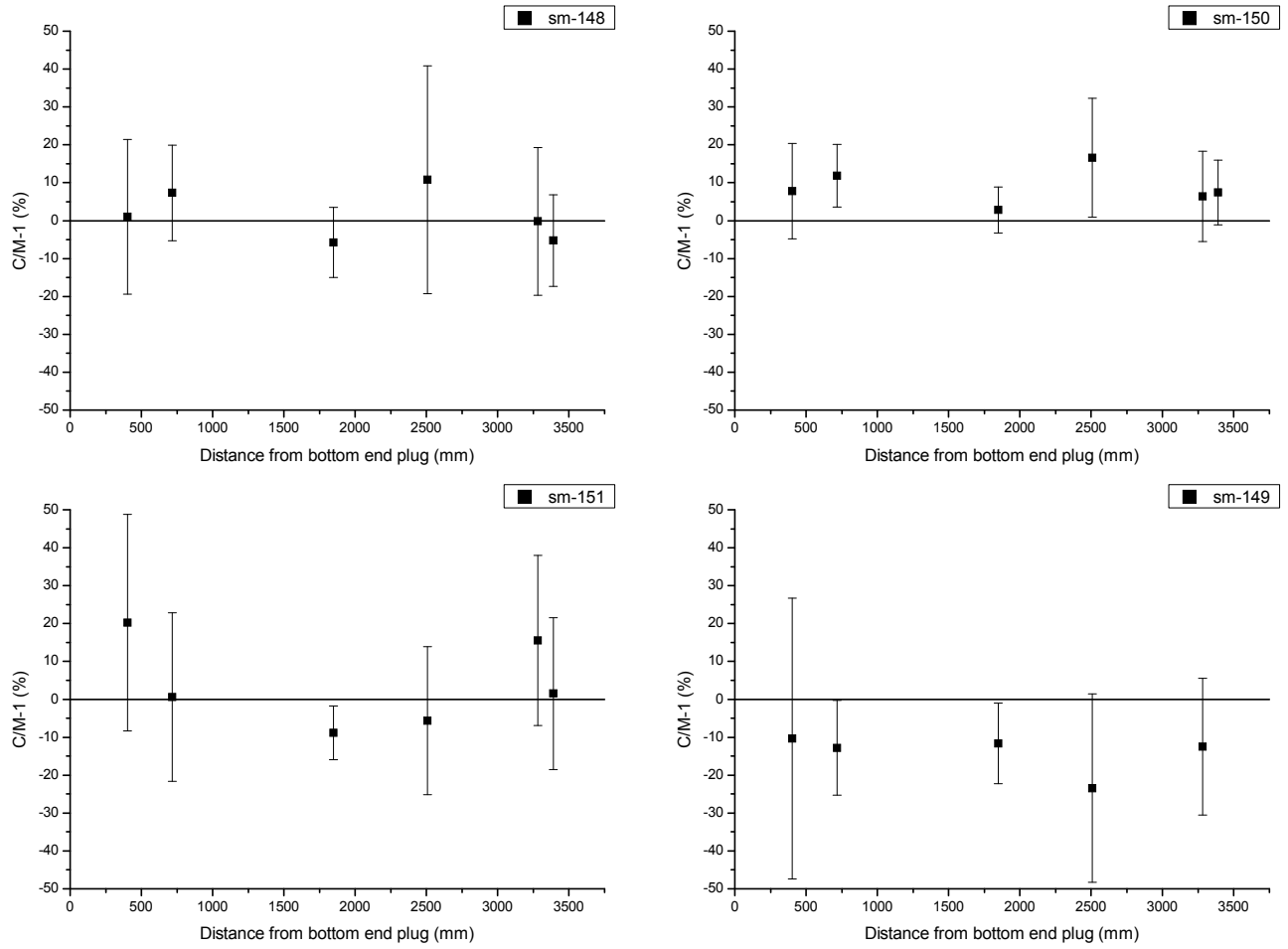
Figure 4-9. Deviations of calculated and measured concentrations for GE14 samples (^{148}Sm, ^{149}Sm, ^{150}Sm, and ^{151}Sm).
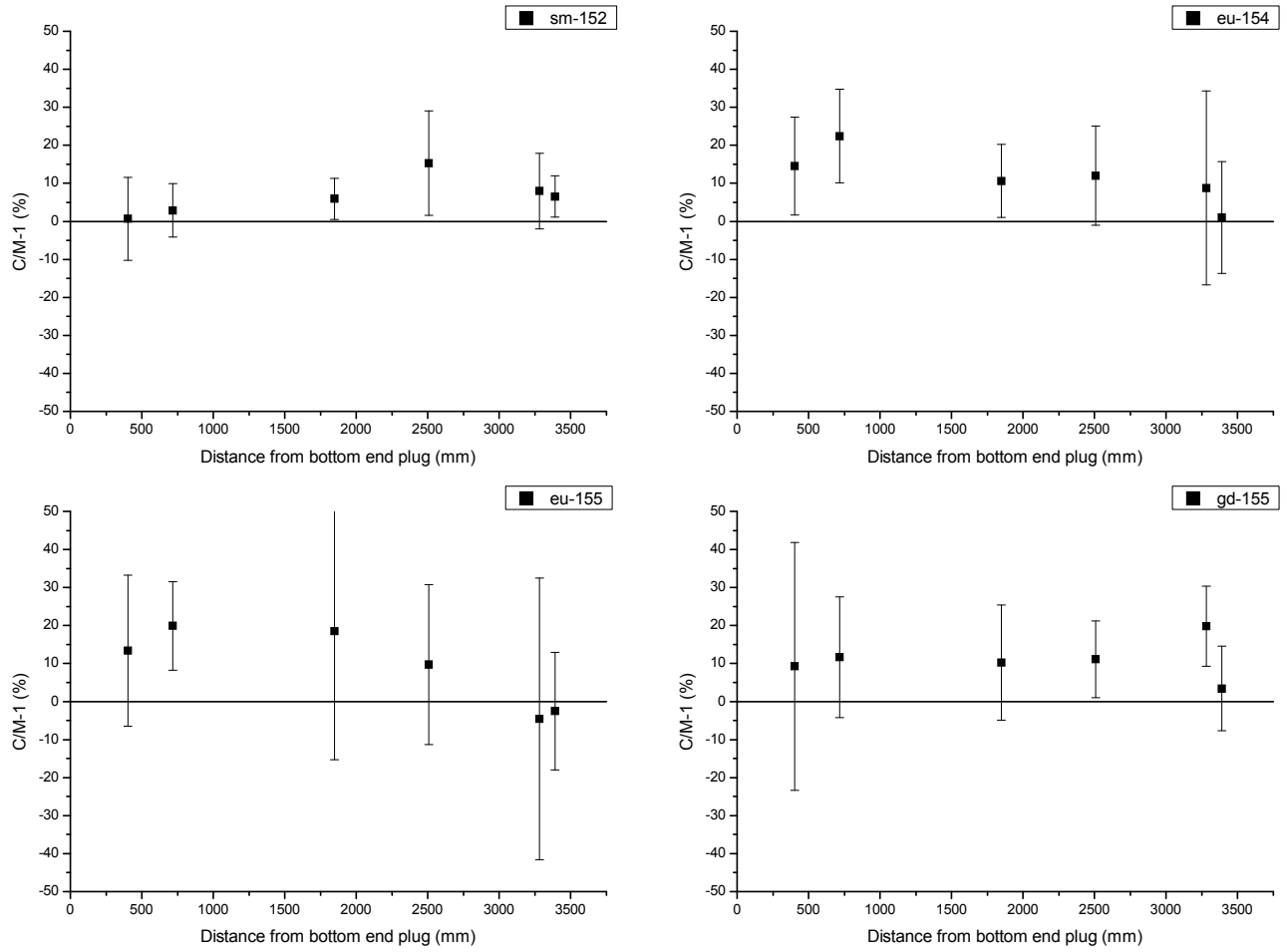
Figure 4-10. Deviations of calculated and measured concentrations for GE14 samples (^{152}Sm, ^{154}Eu, ^{155}Eu, and ^{155}Gd).
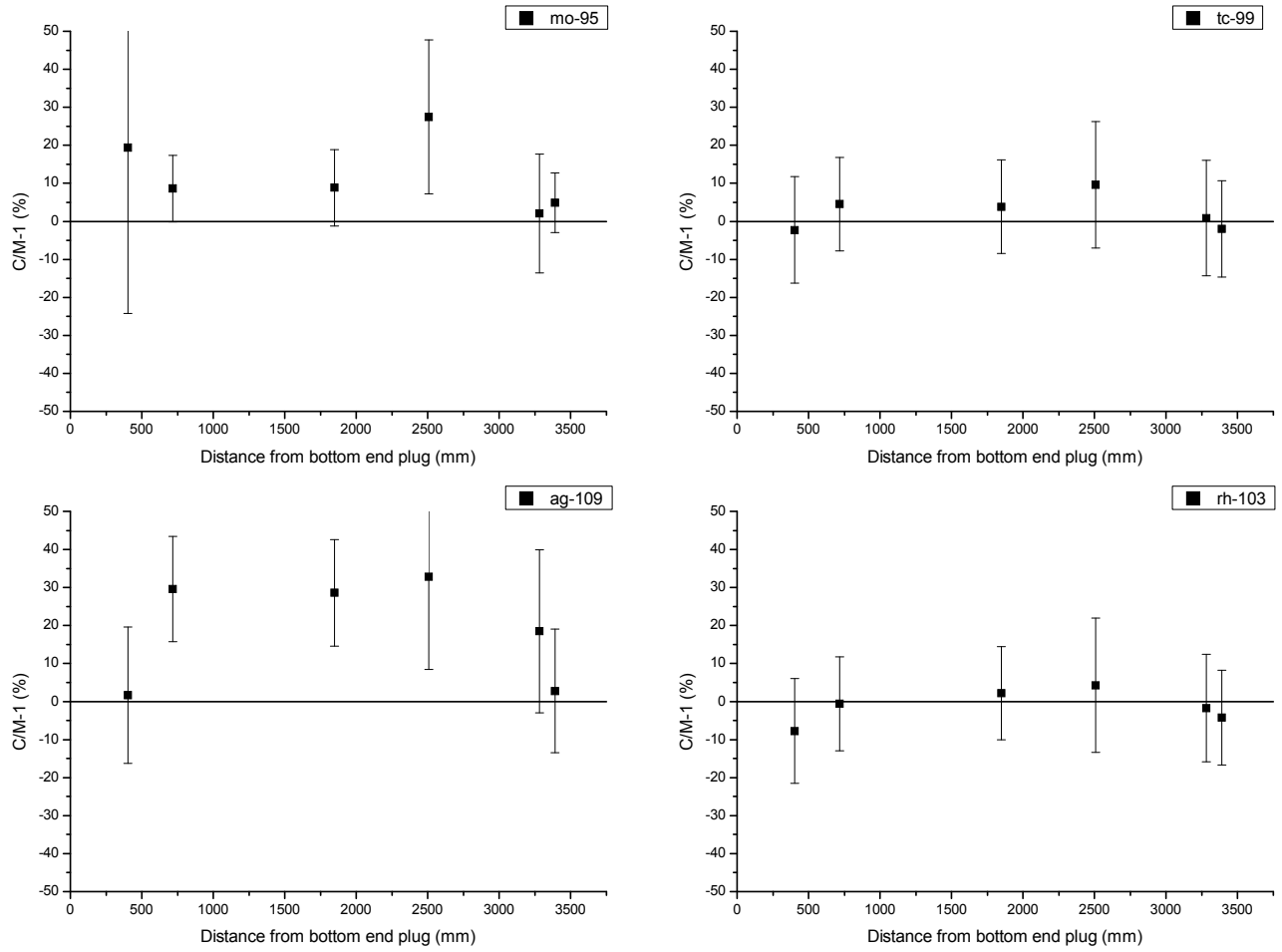
Figure 4-11. Deviations of calculated and measured concentrations for GE14 samples (^{95}Mo, ^{99}Tc, ^{103}Rh, and ^{109}Ag).

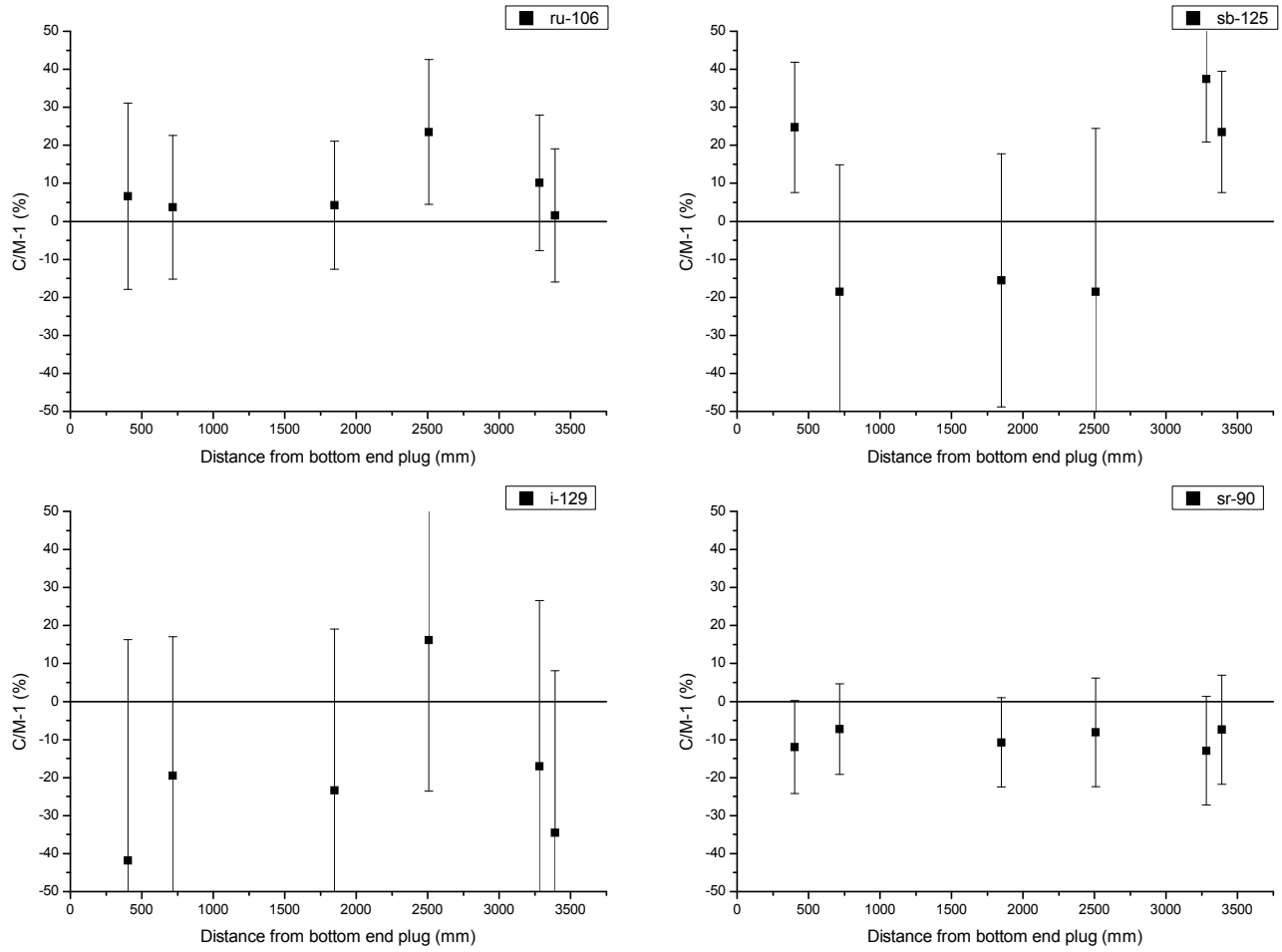**Figure 4-12. Deviations of calculated and measured concentrations for GE14 samples (^{90}Sr, ^{125}Sb, ^{129}I, and ^{106}Ru).**

5. SUMMARY

This report describes recently acquired radiochemical assay data for high burnup fuel obtained from modern BWR assembly designs. These experiments provide important data for validating the computational models used to calculate fuel isotopic concentrations required for reactor and spent nuclear fuel safety studies. The measurements were performed on three spent fuel samples selected from a fuel rod of a SVEA-96 Optima (10×10) assembly irradiated in the Leibstadt reactor in Switzerland, and six samples from a GE14 (10×10) assembly irradiated in the Swedish Forsmark 3 reactor. At this time, only one of the three Leibstadt samples was considered for code validation. The samples were taken from different axial elevations of the assemblies, representing a wide range of void levels and regions of both the dominant (full lattice) and vanished (partial lattice) zones of the assembly. The fuel samples applied in the current study cover a burnup range from 38 to 60 GWd/MTU.

The measurement data represent an important contribution to code benchmarking for modern BWR assembly designs and operating characteristics representative of currently operating reactors. Measurements include isotopes that have not been previously reported in open-source publications for BWR fuels, including all fission products currently considered in burnup credit for nuclear criticality safety.

The measurements are applied in this report to validate the SCALE nuclear safety analysis code system and detailed computational models developed for simulating the SVEA-96 and GE14 assembly designs. Creating the accurate TRITON models for these assemblies involved a significant effort due to the highly heterogeneous and complex assembly design and operating histories. In particular, the large variations in power and moderator void conditions during irradiation required detailed modeling of the time-dependent input quantities. It was found that some default parameters calculated internally by the code were not sufficiently accurate for these designs. Notably, the default Dancoff factors, calculated automatically by SCALE for resonance cross-section generation corrections, were found to be inadequate for these heterogeneous lattice configurations. In this benchmark study, Dancoff factors were calculated externally by Monte Carlo methods and were used to override the default values. The ability to supply time-dependent Dancoff factors as the void changes during irradiation is not an option implemented in TRITON. Updating the input to account for void changes therefore required a complex procedure to *boot strap* separate irradiation cases developed for each individual cycle, with compositions from one case being passed to the next case via intermediate fuel composition files. This study highlighted a number of future code development areas for accurate modeling of complex BWR fuel assemblies.

The comparisons of calculated concentrations with measurements are provided for more than 60 measured nuclides. These experimental uncertainties include a direct component—the reported measurement uncertainties for each nuclide—and an indirect component due to burnup uncertainty. The burnup uncertainty affects each nuclide differently. For example, at high burnup levels a 1% change in the burnup causes a 6% change in the ^{235}U concentration. The uncertainty in the burnup of the sample is therefore an important factor in judging the overall quality of the measurement data.

The results for the SVEA-96 sample (KLU1) measured under the MALIBU extension program are described in Section 4. The comparisons include very high precision measurements performed independently at PSI and SCK•CEN. The calculated results for sample KLU1 are based on a sample burnup determined using the ^{148}Nd concentration measured by PSI, as this result had a smaller experimental uncertainty than the measurement at SCK•CEN. The results show good agreement for the ^{235}U and ^{239}Pu concentrations, and most of the measured fission products.

The results for the GE14 samples measured under the ENUSA program are also described in Section 4. These measurements were performed at Studsvik Nuclear AB. The measurement uncertainties are generally much larger than those observed in the MALIBU program. In particular, the uncertainty in the ^{148}Nd concentrations resulted in significant overall uncertainties in the comparisons of calculations and measurements. The lower precision of Studsvik ICPMS measurements is partly compensated by a larger number of analyses and masses and the availability of multiple burnup indicators.

The GE14 results show generally good and consistent agreement for the uranium and plutonium isotope concentrations, with most calculated results in agreement with the measurements within the experimental uncertainty. Although the differences for some nuclides are large, it is important to consider the overall uncertainty associated with the measurements. In most cases the large deviations are within the range of the experimental uncertainty.

The results for sample 4 (2500 mm elevation) may be improved by including more details of the assembly for the model of this region. The elevation of this sample corresponds to the plenum region near the transition height from the dominant to vanished region of the assembly. This region contains additional hardware not included in the model. Further studies to refine the neutronic representation in this region of the assembly are recommended and may improve the results for this sample.

It is instructive to compare the bias and uncertainties in calculated nuclide concentrations for modern BWR assembly designs evaluated in this report, with uncertainties determined in previous PWR validation studies [11] using the same code methods and nuclear data. The average results for PWR fuel, obtained using 92 fuel samples for a wide range of fuel designs, enrichments, and burnups, are listed in Table 5-1. These results are compared with the weighted average of the six GE14 samples from the ENUSA program and the single SVEA-96 sample from the MALIBU extension program. For the SVEA-96 sample, the standard deviations associated with the measurements are listed. The results for GE14 and SVEA-96 were not combined as the results were significantly different for some nuclides.

The uranium results in Table 5-1 are generally consistent between the PWR data and the BWR results obtained in this present study. The agreement between calculations and the SVEA-96 measurements are observed to be very consistent with previously reported PWR results. However, the plutonium results for the GE14 fuel show differences for most isotopes. For example, ^{239}Pu is overpredicted by about 4% on average for the PWR and SVEA-96 experiments, but is underpredicted on average by about 2% for the GE14 experiments. However, this experiment included samples from high void regions of the lattice, not included in the other experiments. The measured rod J8 is also located at the periphery of the assembly, with an adjacent burnable poison rod and empty lattice positions (in the vanished region), presenting additional heterogeneity and modeling complexities. Because the local conditions in the vicinity of the measured rod are difficult to predict, local uncertainties will introduce additional modeling errors and bias in the calculated results. Consequently, the bias and uncertainties associated with local fuel rod predictions for heterogeneous BWR assembly designs are expected to be typically larger than for PWR designs, which are characterized by much more uniform neutronic conditions.

At this time, both the MALIBU extension program and the ENUSA experimental program are continuing and are commercially restricted. However, it is anticipated that the data will be made public in the future and will provide an important benchmark that can be used to validate other codes, computational models, and nuclear data. The experimental programs are expected to be completed with final recommendations issued in 2013. Based on the outcome and final recommendations, some results presented in this report may be revised as additional information is acquired, particularly updated information on sample burnup and burnup uncertainties. However, no significant changes in the assessment of overall code performance are expected.

Table 5-1. Summary of results for SVEA-96 and GE14 samples

Isotope	PWR			BWR GE14			BWR SVEA-96		
	No. of samples	$(C/M)_{avg}$	σ	No. of samples	$(C/M)_{avg}$	σ	No. of samples	C/M	σ
^{234}U	55	1.124	0.176	6	0.989	0.042	1	1.007	0.009
^{235}U	92	1.012	0.035	6	0.981	0.101	1	1.034	0.024
^{236}U	77	0.981	0.035	6	0.958	0.018	1	0.963	0.004
^{238}U	92	0.999	0.004	6	0.995	0.003	1	0.988	0.004
^{238}Pu	77	0.883	0.059	6	0.860	0.048	1	0.880	0.052
^{239}Pu	92	1.041	0.035	6	0.980	0.018	1	1.043	0.009
^{240}Pu	92	1.022	0.034	6	1.073	0.032	1	1.010	0.009
^{241}Pu	92	0.986	0.045	6	0.969	0.015	1	1.023	0.009
^{242}Pu	91	0.941	0.061	6	0.997	0.059	1	0.925	0.013
^{237}Np	36	1.039	0.195	6	1.034	0.036	1	1.141	0.050
^{241}Am	39	1.102	0.207	6	1.075	0.021	1	1.045	0.028
^{243}Am	38	1.029	0.140	6	1.123	0.179	1	1.076	0.029
^{90}Sr	15	0.991	0.069	6	0.900	0.026	1	0.987	0.020
^{99}Tc	20	1.152	0.154	6	1.012	0.032	1	1.353	0.042
^{101}Ru	7	1.058	0.123	6	0.908	0.032	1	1.163	0.038
^{106}Ru	31	1.079	0.227	6	1.051	0.032	1	0.980	0.106
^{103}Rh	8	1.091	0.109	6	0.978	0.038	1	1.235	0.039
^{109}Ag	6	1.773	0.746	6	1.183	0.135	1	1.357	0.046
^{125}Sb	18	1.996	0.466	6	1.221	0.256	1	1.261	0.064
^{133}Cs	10	1.019	0.017	6	0.929	0.039	1	1.020	0.015
^{134}Cs	59	0.930	0.071	6	0.883	0.052	1	1.110	0.015
^{135}Cs	16	1.027	0.037	6	0.992	0.010	1	1.010	0.017
^{137}Cs	73	0.993	0.031	6	0.954	0.032	1	1.001	0.015
^{143}Nd	36	1.008	0.032	6	1.082	0.019	1	1.047	0.003
^{145}Nd	36	0.995	0.022	6	1.026	0.027	1	0.975	0.005
^{148}Nd	77	1.006	0.014	6	1.000	0.001	1	1.002	0.007
^{144}Ce	32	0.979	0.081	6	0.861	0.177	1	0.884	0.156
^{147}Sm	24	1.016	0.034	6	1.000	0.139	1	1.010	0.013
^{149}Sm	20	1.019	0.062	6	0.879	0.011	1	0.934	0.232
^{150}Sm	24	1.008	0.032	6	1.065	0.032	1	1.046	0.010
^{151}Sm	24	0.979	0.044	6	0.958	0.118	1	1.016	0.010
^{152}Sm	24	1.016	0.037	6	1.053	0.030	1	0.992	0.010
^{153}Eu	19	0.991	0.031	6	1.111	0.061	1	1.061	0.014
^{154}Eu	44	1.042	0.104	6	1.124	0.079	1	1.134	0.014
^{155}Eu	11	0.956	0.077	6	1.117	0.117	1	1.072	0.017
^{155}Gd	19	0.916	0.144	6	1.116	0.059	1	1.154	0.050

6. REFERENCES

1. *SFCOMPO – Spent Fuel Isotopic Composition Database*. http://www.oecd-nea.org/sfcompo/

2. D. Boulanger, M. Lippens, L. Mertens, J. Basselier, and B. Lance, "High Burnup PWR and BWR MOX Fuel Performance: A Review of Belgonucleaire Recent Experimental Programs," *Proc. Int. Mtg. LWR Fuel Performance,* Orlando, Florida, September 19–22, 2004, American Nuclear Society, 2004.

3. J. M. Conde, J. M. Alonso, J. A. Gago, P. González, M. Novo, and L. E. Herranz, "Spanish R&D Program on Spent Fuel Dry Storage," *Trans. International Meeting on LWR Fuel Performance, Top Fuel 2006*, Salamanca, Spain (2006).

4. *SCALE 6.1: A Comprehensive Modeling and Simulation Suite for Nuclear Safety Analysis and Design*. Available from Radiation Safety Information Computational Center at Oak Ridge National Laboratory as CCC-785.

5. *10×10 SVEA Fuel Critical Power Experiments and CPR Correlations: SVEA-96*, ABB Combustion Engineering Nuclear Power, Inc., CENPD-392-NP (1999).

6. *ARIANE International Programme—Final Report*, ORNL/SUB/97-XSV750-1, Oak Ridge National Laboratory, Oak Ridge, Tennessee (May 1, 2003).

7. L. E. Fennern, *ABWR Seminar – Reactor, Core & Neutronics*, GE Energy / Nuclear, April 13, (2007).

8. M. D. DeHart and S. M. Bowman, "Reactor Physics Methods and Analysis Capabilities in SCALE," *Nuclear Technology* **174**(2), 196 (2011).

9. M. L. Williams, "Resonance Self-Shielding Methodologies in SCALE 6," *Nuclear Technology*, **174**(2), 149 (2011).

10. H. J. Smith, "Modeling Depletion Simulations for a High-Burnup, Highly Heterogeneous BWR Fuel Assembly with SCALE," *Proc. of PHYSOR 2012: Advances in Reactor Physics,* Knoxville, Tennessee, April 15–20, 2012.

11. G. Ilas, I. C. Gauld, and G. Radulescu, "Validation of new depletion capabilities and ENDF/B-VII data libraries in SCALE," *Annals of Nuclear Energy* **46,** 43–55 (2012).

U.S. NUCLEAR REGULATORY COMMISSION

BIBLIOGRAPHIC DATA SHEET

(See instructions on the reverse)

1. REPORT NUMBER
(Assigned by NRC, Add Vol., Supp., Rev., and Addendum Numbers, if any.)

NUREG/CR-7162
ORNL/TM-2013/18

2. TITLE AND SUBTITLE

Analysis of Experimental Data for High Burnup BWR Spent Fuel Isotopic Validation— SVEA-96 and GE14 Assembly Designs

3. DATE REPORT PUBLISHED

MONTH	YEAR
03	2013

4. FIN OR GRANT NUMBER

NRC JCN N6540

5. AUTHOR(S)

H. J. Smith, I. C. Gauld, and U. Mertyurek

6. TYPE OF REPORT

Technical

7. PERIOD COVERED (Inclusive Dates)

8. PERFORMING ORGANIZATION - NAME AND ADDRESS (If NRC, provide Division, Office or Region, U. S. Nuclear Regulatory Commission, and mailing address; if contractor, provide name and mailing address.)

Oak Ridge National Laboratory
Managed by UT-Battelle, LLC
Oak Ridge, TN 37831-6170

9. SPONSORING ORGANIZATION - NAME AND ADDRESS (If NRC, type "Same as above", if contractor, provide NRC Division, Office or Region, U. S. Nuclear Regulatory Commission, and mailing address.)

Division of Systems Analysis
Office of Nuclear Regulatory Research
U. S. Nuclear Regulatory Commission
Washington, DC 20555–0001

10. SUPPLEMENTARY NOTES

11. ABSTRACT (200 words or less)

This report describes experimental radiochemical assay data, recently acquired under two international collaboration programs, for the isotopic compositions in high burnup spent nuclear fuel from modern boiling water reactor (BWR) assemblies. The Belgian MALIBU extension program provides measured data for isotopic contents of more than 50 nuclides in spent fuel samples selected from a SVEA-96 (10×10) Optima fuel assembly with burnups between 59 and 63 GWd/MTU. An experimental program in Spain provides additional isotopic data for more than 60 nuclides in samples selected from a GE14 (10×10) fuel assembly that cover a burnup range 38 to 56 GWd/MTU. These samples represent a wide range of moderator void conditions. The measurement data include concentrations of actinides and fission products important to nuclear decay heat, radiological sources, and nuclear criticality safety. These data are of essential for validation of the computational models used to calculate fuel isotopic concentrations and activities applied in reactor and spent nuclear fuel safety studies. Computational benchmark analyses using the measurements are performed using the the SCALE 6.1 computer code system. These measurements represent an important contribution to the code benchmark database by providing data for modern BWR assembly designs and operating conditions representative of currently operating reactors.

12. KEY WORDS/DESCRIPTORS (List words or phrases that will assist researchers in locating the report.)

SCALE, BWR, SVEA-96, GE14, spent nuclear fuel, isotopic data, radiochemical analysis, MALIBU, ENUSA, TRITON, ORIGEN, validation, burnup credit

13. AVAILABILITY STATEMENT

unlimited

14. SECURITY CLASSIFICATION

(This Page)

unclassified

(This Report)

unclassified

15. NUMBER OF PAGES

16. PRICE

Analysis of Experimental Data for High Burnup BWR Spent Fuel
Isotopic Validation – SVEA-96 and GE14 Assembly Designs

March 2013